CHARACTERIZATION OF LOCAL FLOW BEHAVIOUR IN CONICAL SPOUTED BEDS

A THESIS SUBMITTED TO
THE GRADUTE SCHOOL OF NATURAL AND APPLIED SCIENCES
OF
MIDDLE EAST TECHNICAL UNIVERSITY

BY

ALİ YENİÇERİ

IN PARTIAL FULFILLMENT OF THE REQUIREMENTS
FOR
THE DEGREE OF MASTER OF SCIENCE
IN
CHEMICAL ENGINEERING

SEPTEMBER 2019

Approval of the Thesis:

CHARACTERIZATION OF LOCAL FLOW BEHAVIOUR IN CONICAL SPOUTED BEDS

submitted by **ALİ YENİÇERİ** in partial fulfillment of the requirements for the degree of **Master of Sciences in Chemical Engineering Department, Middle East Technical University** by,

Prof. Dr. Halil Kalıpçılar
Dean, Graduate School of **Natural and Applied Sciences** _____

Prof. Dr. Pınar Çalık
Head of the Department, **Chemical Engineering** _____

Prof. Dr. Görkem Külah
Supervisor, **Chemical Engineering Dept., METU** _____

Examining Committee Members:

Prof. Dr. Murat Köksal
Mechanical Engineering Dept., Hacettepe University _____

Prof. Dr. Görkem Külah
Chemical Engineering Dept., METU _____

Asst. Prof. Dr. Özgür Ekici
Mechanical Engineering Dept., Hacettepe University _____

Assoc. Prof. Dr. Erhan Bat
Chemical Engineering Dept., METU _____

Asst. Prof. Dr. İnci Ayrancı
Chemical Engineering Dept., METU _____

Date: 03.09.2019

I hereby declare that all information in this document has been obtained and presented in accordance with academic rules and ethical conduct. I also declare that, as required by these rules and conduct, I have fully cited and referenced all material and results that are not original to this work.

Name, Surname: Ali Yeniçeri

Signature:

ABSTRACT

CHARACTERIZATION OF LOCAL FLOW BEHAVIOUR IN CONICAL SPOUTED BEDS

Yeniçeri, Ali
M.Sc., Department of Chemical Engineering
Supervisor: Prof. Dr. Görkem Külah

September 2019, 83 pages

Conical spouted beds are used in various physical and chemical applications such as drying, coating, and pyrolysis of waste plastic and biomass owing to their effective feature of gas-solid contact. To design and operate these units in high efficiency, a complete understanding of the phenomena and detailed investigation of local flow structure are of paramount importance. In this study, the effects of bed design parameters (unit size, conical angle, spouting gas-inlet diameter) and operational conditions (particle density, axial position) on bed local flow structure were investigated in detail. Experiments were performed in small and large conical spouted beds by using light and heavy particles with varying density (2460 kg/m^3 $\leq$ ρ_p $\leq$ 6050 kg/m^3). To observe the effects on local flow structure, an optical probe system was used. Additionally, an empirical correlation was proposed to predict the solids hold-up at the spout center (r = 0) for light and heavy particles.

The investigated parameters caused significant changes in spout region while the annulus region was found to be unaffected. The particle velocity decreased and solids hold-up and particle flux increased from the bed bottom to the bed surface. Using larger gas-inlet diameter decreased the particle flux in the spout. An increase in cone

angle caused a major decrease in particle flux. Introducing fluidizing gas through the conical section to the system caused minimal effect on particle flux, resulting in only 8% increase in the spout region. Particle velocity and solids hold-up did not significantly change in presence of fluidizing gas.

Keywords: Conical spouted bed, spout-fluid bed, optical probe, local flow structure, high-density particles

ÖZ

KONİK TAŞKIN YATAKLARDA YEREL AKIŞ DAVRANIŞININ KARAKTERİZASYONU

Yeniçeri, Ali
Yüksek Lisans, Kimya Mühendisliği Bölümü
Tez yöneticisi: Prof. Dr. Görkem Külah

Eylül 2019, 83 sayfa

Konik taşkın yataklar, etkili gaz-katı temas özelliklerinden dolayı, kurutma, kaplama ve biyoyakıt ile plastik atıkların pirolizi gibi çeşitli fiziksel ve kimyasal uygulamalarda kullanılır. Bu üniteleri tasarlamak ve yüksek verimde çalıştırmak için olayın baştan sona anlaşılması ve yerel akış davranışının detaylı bir biçimde araştırılması çok önemlidir. Bu çalışmada, yatak tasarım parametrelerinin (ünitenin boyutu, konik açısı, taşkınlaşma gazının giriş çapı) ve işletim koşullarının (parçacık öz kütlesi, eksenel pozisyon) yatak içerisindeki yerel akış yapısı üzerindeki etkileri detaylı bir şekilde incelenmiştir. Deneyler küçük ve büyük ölçekli konik taşkın yataklarda çeşitli öz kütleli hafif ve ağır parçacıklar ($2460\ kg/m^3 \leq \rho_p \leq 6050\ kg/m^3$) kullanılarak gerçekleştirilmiştir. Yerel akış yapısındaki etkileşimi gözlemlemek için optik sonda sistemi kullanılmıştır. Ek olarak, bu deneysel veriler kullanılarak taşkın bölge merkezindeki ($r = 0$) hafif ve ağır parçacıkların konsantrasyonu için tahmin yapmak adına ampirik bir korelasyon oluşturulmuştur.

İncelenen parametreler taşkın bölgede önemli ölçüde değişikliklere sebep olmuşken, parametrelerin halka bölgesi üzerinde ise etkisiz olduğu gözlemlenmiştir. Yatak içerisinde yatak tabanından yatak yüzeyine gidildikçe parçacık hızı azalmışken,

parçacık konsantrasyonu ve parçacık akısı ise artış göstermiştir. Taşkınlaşma gazı giriş çapını büyütmek parçacık akısını taşkın bölgede azaltmıştır. Yatak konik açısındaki artış parçacık akısında büyük bir düşüşe sebep olmuştur. Sisteme konik kısımdan akışkanlaşma gazı beslemek parçacık akısı üzerinde, taşkın bölgedeki %8'lik artışı baz alarak düşük bir artışa sebep olmuştur. Parçacık hızı ve konsantrasyonu ise akışkanlaşma gazı varlığında kayda değer bir değişim göstermemiştir.

Anahtar kelimeler: Konik taşkın yatak, taşkın akışkan yatak, optik sonda, yerel akış yapısı, yüksek öz kütleli parçacıklar

Dedicated to My Beloved Family…

ACKNOWLEDGEMENT

I would like to thank sincerely to my supervisor Prof. Dr. Görkem Külah and I would like to express my gratitude to Prof. Dr. Murat Köksal for their guidance, support, suggestions and more importantly, motivation throughout this study.

I would like to give my special thanks to our invaluable technician, Hasan Çelikli, for his aids, technical supports and friendship.

I extend my gratitude to my colleagues Onur Yaman, Chiya Sawari, and Shahab Golshan and Neslin Güler for their advices and precious friendships in this study.

Lastly, I feel the deepest gratitude and send my best thanks to each and every member of my beloved family, for their encouragement, endless support and purest love throughout my thesis.

This study was supported by the Scientific and Technological Research Council of Turkey (TUBITAK) as project numbered '115M392'.

TABLE OF CONTENTS

LIST OF TABLES

TABLES

LIST OF FIGURES

FIGURES

LIST OF SYMBOLS

SYMBOLS

a_σ	Variance interval coefficient, -
A	Lower limit for cross-correlation coefficient, -
C	Cross covariance function, -
d_p	Particle diameter, mm
D_c	Cylindrical diameter, mm
D_i	Gas-inlet diameter, mm
D_o	Cone bottom diameter, mm
E	Hydrodynamic coefficient, -
f_d	Rotating frequency of chopper disc,
G_s	Particle flux, kg/m^2s
H_b	Static bed height, mm
H_c	Conical section height, mm
I_1 (t)	Voltage signal of first channel at t period, volt
I_2 (t+τ)	Voltage signal of second channel at t+τ period, volt
L_e	Effective distance, mm
N	Data number, -
Q_0	Superficial gas flow rate, m^3/min
Q_f	Fluidizing gas flow rate, m^3/min
Q_{min}	Minimum fluidizing gas flow rate, m^3/min

Q_{max}	Maximum fluidizing gas flow rate, m^3/min
Q_{ms}	Minimum spouting gas flow rate, m^3/min
Q_t	Total gas flow rate, m^3/min
r	Radial distance, mm
r_d	Distance of optical probe tip to chopper disc center, mm
r_s	Spout radius, mm
R_{xy}	Cross-correlation coefficient, -
$R_{xy,down}$	Downward Cross-correlation coefficient, -
$R_{xy,max}$	Maximum Cross-correlation coefficient, -
$R_{xy,up}$	Upward Cross-correlation coefficient, -
S_d	Angular velocity of chopper disc, m/s
T	Sampling period, s
U_0	Superficial gas velocity, m/s
U_{ms}	Minimum spouting velocity, m/s
U_p	Particle velocity, m/s
V	Measured voltage signal, volt
V_b	Voltage of original particles, volt
V_c	Voltage of black particles, volt
W_p	Solid flow rate, kg/s
X_b	Volume fraction of original particles, -
X_c	Volume fraction of black particles, -
Y	Mass fraction of particles, -
z	Axial height, mm

Greek Symbols

ΔP	Bed pressure drop, Pa
γ	Angle of the conical section, degree
ε	Local bed voidage, -
ε_0	Loosely packed bed voidage, -
ε_s	Local solids hold-up, -
$\varepsilon_{s,0}$	Loosely packed solids hold-up, -
$\varepsilon(0)$	Bed voidage at the spout center, -
$\varepsilon(w)$	Bed voidage at the wall, -
ρ_p	Particle density, kg/m^3
ρ_g	Density of glass beads, kg/m^3
φ	Sphericity, -
τ	Time delay, s

ABBREVIATIONS

ABBREVIATIONS

EPS Expanded Polystyrene

MFC Mass Flow Controller

NA Not available

PE Polyethylene

PP Polypropylene

CHAPTER 1

INTRODUCTION

In most of industrial applications based on multiphase systems, the intimate contact of the phases with each other is aimed for a feasible outcome. Many different techniques have been developed in order to ensure this intimate contact between the phases.

The phenomenon of fluidization is designated and utilized in multiphase systems due to its effective phase-interaction. Basically, this system forms when sufficient amount of fluid is upwardly passed through a bed filled with fine particles. By means of this fluid, all particles are fluidized. Despite several features of fluidized bed such as perfect mixing between the phases and circulation system availability, fluidized beds are seen to be inconvenient for handling dense or large particles. This type of particles (Type-D in Geldart's categorization) require higher fluid flow rate in order to be fluidized. In gas-solid systems, this may cause gas bubbles to coalesce and to become larger whose diameter can reach even the size of the column diameter, and thereby slugging may occur. As they occupy big volumes inside the bed, the expected intimate contact can be precluded which results in poor reaction efficiency. Owing to inconsistent particle agitation, fluidized bed system becomes ineffective for fluid-solid contact for large and dense solid particles (Kunii and Levenspiel, 1991).

Mathur and Gishler (1955) established a new technique in order to prevent this problem for coarse and dense particles. In this technique, the gas is vertically supplied through a small nozzle placed at the center. With the sufficient gas feed, the

flow is strong enough to aerate particles which are positioned at the bottom, and a small gas channel occurs in the axial direction. Upcoming particles together with the gas reach to surface and form a fountain. These particles are then scattered from the center depending on the trajectory that the gas follows and by means of gravity they fall down to the region between the gas channel and bed wall. The void formed by the particles repelling of the gas is occupied by new particles coming around the jet and are gone adrift. Particles at the surface have a slow downward-inward motion and ultimately affiliated to the flow. Such a flow pattern provides a toroidal-like circulation throughout the bed. This system is called *Spouted Bed* as shown in **Figure 1.1**. Aforementioned flow and particle pattern distinguish the overall bed into two different sections; s*pout* and *annulus. Spout region* is the place where the internal jet is formed by gas feed that pushes the lean particle phase in upward direction with high velocity. Upcoming particles emerge to the surface, randomly scatter from the center and then rain back to the *annulus region* where the dense phase of particles slowly move down to the center. As the supplied gas rises up and particles fall down, the overall circulation is completed. By its unique flow behaviour, spouted beds are used in pyrolysis, catalytic reactions, granulation and coating (Epstein and Grace, 2011).

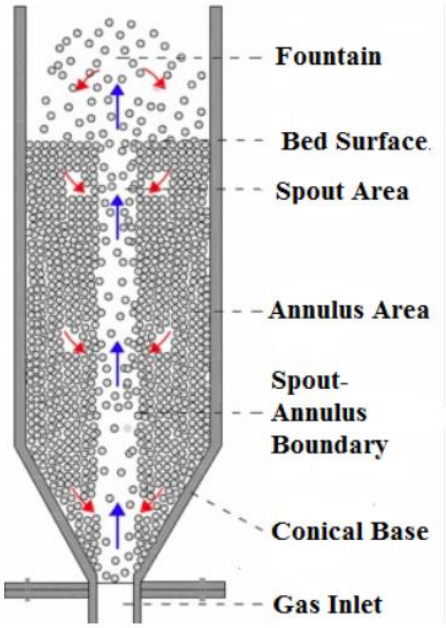

Figure 1.1 Conventional Spouted Bed (Ali et al., 2016)

Since an efficient gas-solid contact is desired in applications, one of the essential factors is the residence time of the gaseous phase. In ultra pyrolysis as a fast reaction application for instance, selectivity is the conditioning factor and so optimum residence time of the gas can be down to milliseconds (Stocker et. al., 1989). Here, the gas residence time being long is a limitation factor for conventional spouted bed. Another disadvantage is limited gas-solid contact considering the dead zones in annulus. In order to overcome these problems, filling the particles up to conical section only is a reasonable option. By this way, the gas residence time can be shortened as its distribution becomes narrow. Furthermore, local mixing performance augments considerably due to less dead-zones in annulus. These systems are named as *Conical Spouted Bed,* shown in **Figure 1.2**, that have been used in applications such as drying, particle coating, polymerization and chemical vapor deposition (Epstein and Grace, 2011).

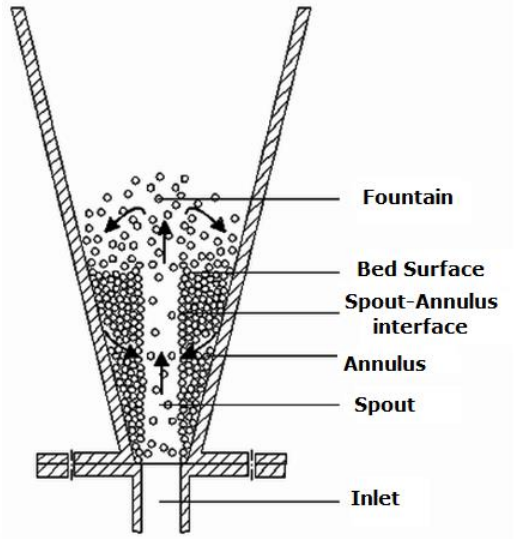

Figure 1.2 Conical Spouted Bed (Elordi et al., 2007)

Conical spouted beds have a feature that the gas velocity at the inlet can be increased essentially without losing the characteristic cyclic movement of the solids. However, the flow rate of gas feed matters for the nature of flow regime in the bed. **Figure 1.3** shows the change of the total pressure drop with increasing and decreasing superficial gas velocity in a conical spouted bed. This curve indicates different flow regimes caused by different inlet gas flow rates. It starts with an almost linearly increasing line which corresponds to rising pressure drop in a packed bed as superficial velocity increases. At the instant that peak value is reached, the gas reaches to the bed surface and harshly emerges among the particles. It is followed by the step of incipient spouting, that is, the entrainment of particles with loosely-packed state at the inlet by the inlet gas feed with high flow rate. The corresponding value of superficial gas velocity is designated as *minimum spouting velocity*, $U_{ms.}$ As the gas velocity further increases, the stable spouting regime is obtained, see **Figure 1.3 (a)**. The small range of fixed pressure drop corresponds to the period of stable increase in fountain height caused by higher gas velocities.

By further increasing the gas velocity, spout region gradually enlarges and intertwines with annulus. The gas burst at the surface becomes stronger and annular region is no longer observable from the bed surface. This state is called *transition state* which is illustrated in **Figure 1.3 (b)**. Further increase in the gas velocity results in the disappearance of annular region completely and there becomes more likely one single region in the bed. Both of gas and particle distribution become almost uniform, leading to a new state called jet spouting regime, shown in **Figure 1.3 (c)**.

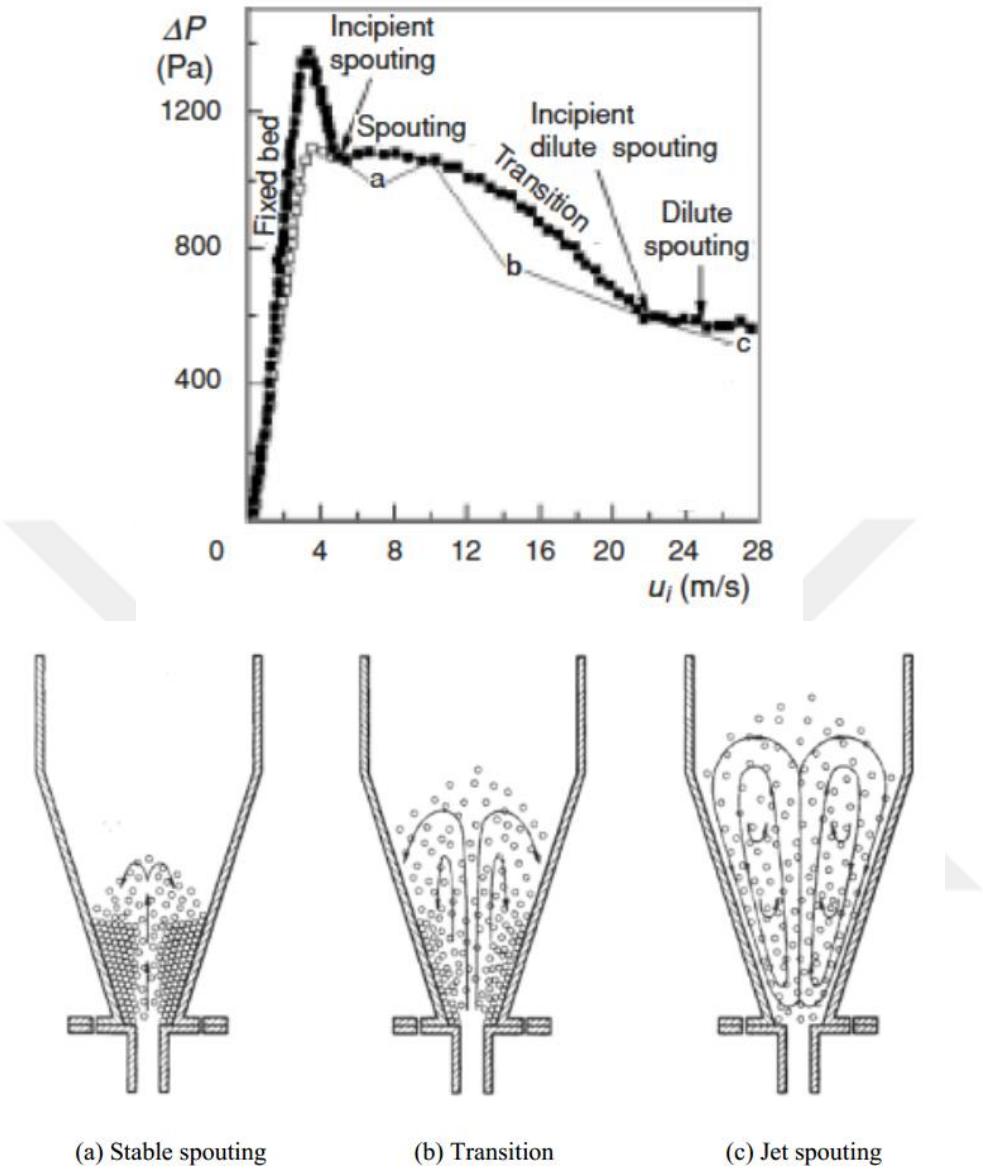

Figure 1.3 Pressure drop − Superficial gas velocity curve and different flow regimes in conical spouted beds (Epstein and Grace, 2011)

In spite of the narrow gas distribution in conical spouted beds, local mixing differences particularly in annulus section and the presence of dead zones constitute a problem. Packed nature in the annulus may cause incidents such as particle agglomeration, adhesion, sticking to bed wall or column base, which also depend on

the operation type and physical/chemical conditions (Epstein and Grace, 2011). To overcome these shortcomings, Chatterjee (1970) developed a new technique named *Spout-Fluid Bed* which is a unique fluid-particle agitated bed including the salient properties of fluidized beds and spouted beds (Chatterjee et al., 1983). In this technique, an auxiliary fluidizing gas in introduced through a perforated distributor (see **Figure 1.4**) which corresponds to the conical lateral surface of the column in addition to spouting gas entering from the central nozzle. Considering its properties, the spout-fluid bed is a successful modification to the conventional spouted bed with a potential of providing higher solid circulation. This is caused by the auxiliary flow through the spout region which increases the radial influx. Consequently, a better gas-solid contact and mixing in annulus region is expected to take place which results in decrease in agglomeration and sticking problems.

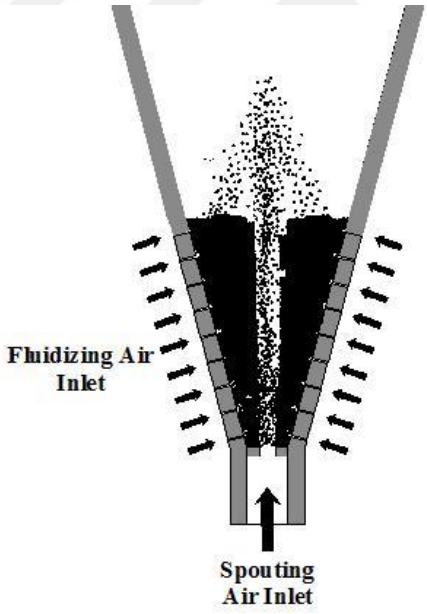

Figure 1.4 Conventional spout-fluid bed (Yaman, 2017)

In order to achieve the highest possible reactor efficiency, it is crucial to understand the bed's overall and local flow behaviour for optimum design and operating conditions. In this regard, many studies (Kmiec, 1980; Choi and Meisen 1992, Olazar et al., 1994; Wang et al., 2004; Duarte et al., 2008; Sarı et al., 2012) in spouted and conical spouted beds are conducted most of which investigated the pressure drop and minimum spouting velocity. As for local flow structure, although several studies (He et al., 1994; Olazar et al., 1995, 1998, 2001; San Jose et al., 1998a, 1998b, 2005, 2006; Wang et al., 2009) evaluated the effects of bed geometry and operating parameters on local flow structure, their results enlightened the flow structure in conical spouted beds operating with light particles only (65 $kg/m^3 \leq \rho_p \leq$ 2400 kg/m^3). Particle density is a prominent parameter having salience influence on bed hydrodynamics. Therefore in order to design and operate high-performance conical spouted beds, it is essential that the effect of bed design parameters and operating conditions on local flow structure in the spouted and spout-fluid beds operating with both light and heavy particles is known in detail. The absence of local flow structure studies in conical spouted and spout-fluid beds operating with high density particles constitutes the keystone of this study.

CHAPTER 2

LITERATURE SURVEY ON LOCAL FLOW STRUCTURE IN CONICAL SPOUTED BEDS AND SPOUT-FLUID BEDS

The “local flow structure” term means particle flow characteristics in the bed and can be monitored by measuring particle velocity, solids hold-up (or particle concentration) and particle flux. Although there are many different techniques such as gamma-ray computer tomography (Ali et al. 2016) or scintillation counter (Van Velzen et al. 1974) to measure these quantities, optical probe system was used in most of the local flow structure studies (Olazar et al., 1995; San Jose et al., 1998; Wang et al., 2009; Santos et al., 2012; Kulah et al., 2016; Aradhya et al., 2017). Due to its design, the optical probe has the ability to simultaneously measure the local instantaneous particle velocity and local solids hold-up. Therefore, optical fibre probes were used in this study to measure both the particle velocity and solids hold-up in conical spouted beds. The literature studies regarding the local flow structure in conical spouted beds are summarized in **Table 2.1 and 2.2**.

Olazar et al. (1995), using glass beads in different sizes, investigated the effects of axial height (height at which the particle velocity is measured) and gas-inlet diameter on particle velocity in a conical spouted bed. They monitored that, an increase in axial height or gas-inlet diameter resulted in a decrease in particle velocity in the spout region. In their next study, Olazar et al. (1998) continued their investigation with the effect of conical angles and observed a direct proportional relation between the particle velocity in the spout region and conical angle. Furthermore, based on

their findings, they proposed a correlation predicting the particle velocity along the spouted bed. In this correlation, the particle velocity is dependent on spouted bed design criteria such as the ratios of d_p/D_o and D_i/D_o. Later, Olazar and co-workers (2001) further investigated the effect of conical angle by using 60°, 120° and 180° conical beds. They again used glass beads and recorded that the particle velocity decreases with increasing cone angle, when the cone angle is beyond 45°. Wang et al. (2009) evaluated the axial height effect on particle velocity and focused on spout and annulus regions together. Their results were similar to the ones obtained by Olazar et al. (1995) for the spout region. They additionally observed that although the particle velocity decreases with increasing axial height, the change is from -0.02 m/s to -0.01 m/s in annulus region which is not significant considering the entire physical system. Santos et al. (2012) used relatively bigger sized (2.2 mm) glass beads in 60° cylindrical spouted bed and investigated the effect of presence of optical probe on fountain height. According to their observations, the insertion of the optical probe causes a disturbance decreasing the fountain height, especially when the optical probe is at the spout center.

There are also studies on the measurement of solids hold-up (San Jose et al., 1998; San Jose et al., 2005; Wang et al. 2009) in the literature. To investigate the effect of particle diameter and cone angle on solids hold-up, San Jose et al. (1998) used 3, 4 and 5 mm diameter glass beads in the same experimental setup of Olazar et al. (1995; 1998; 2001). According to their results, the solids hold-up in the spout region increased with increasing axial height. They observed that the solids hold-up had a slight increase of 0.01 at the spout axis, as the cone angle increases from 33° to 45°, while the particle diameter demonstrated no significant effect on solids hold-up. Using the experimental data they obtained from the tests with glass beads, San Jose and co-workers (1998) proposed an empirical correlation which predicts the solids hold-up at the spout axis, at the bed wall and at any radial distance. To investigate the effect of particle density, San Jose et al. (2005) conducted experiments with expanded polystyrene (ρ_p = 65 kg/m^3), polypropylene (ρ_p = 890 kg/m^3), low-density polyethylene (ρ_p = 923 kg/m^3), high-density polyethylene (ρ_p = 930 kg/m^3) and

extruded polystyrene (ρ_p = 1030 kg/m^3) together with glass beads (ρ_p = 2420 kg/m^3). Although they observed that solids hold-up increased with increasing particle density in the spout region, there was no trend in the annulus region. In addition, they improved the earlier correlation for prediction of local solids hold-up (San Jose et al., 1998) by including the lighter particles together with glass beads.

Solid circulation inside the bed is one of the foremost parameters to check. In this regard, San Jose et al. (2006) measured the velocity of the same particles used in San Jose et al. (2005) to calculate particle cross-flow and determine their trajectories. They found that particle circulation in the spout region changes with particle density. However, this change does not follow a trend. In the annulus, the particle velocity is increasing with decreasing particle density.

Although many different particles such as wheat, millet, silica sand, glass beads, polyethylene and polystyrene (Sutanto et al., 1985; Berruti et al., 1988; Nagashima et al., 2015; Pianarosa et al., 2000; San Jose et al., 2005) were used in the literature, they were all light particles, glass beads being the maximum. In order to have a broader perspective and also to be able to investigate relevant industrial applications, where high –density particles are used, studies should be expanded. This necessitates the examination of the effect of high-density particles on local particle flow in order to observe and evaluate the flow behavior throughout the bed from a broader perspective. In this respect, it will be possible to increase the yield.

Regarding the high-density particles in cylindrical and conical spouted bed systems, Kulah et al. (2016) performed the first study investigating the local flow structure with zirconia particles (ρ_p = 6050 kg/m^3). They reported that the particle velocity in the spout decreased with increasing axial height, but no change was observed with the change in conical angle. Solids hold-up was found to increase with increasing axial height, decreasing particle diameter, and decreasing cone angle. As for particle flux, it was found to be directly proportional to axial height and static bed height, while inversely proportional to cone angle and particle diameter. In another study conducted with heavy particles, steel beads were used by Ali et al. (2016) and

Aradhya et al. (2017) in a cylindrical spouted bed system. Rather than local flow structure, they focused on scale-up methodology in spouted beds. Therefore a direct comparison of glass and steel beads was out of the scope of their study. Although these studies shed some light to the local flow behavior for high-density particle systems to some extent, they were conducted in small-scale spouted beds (D_c = 76, 152 mm). Therefore, this thesis was done as an extension of previous studies, by investigating local flow structures in both small and large scale (D_c = 250 mm) conical spouted beds operating with three different particles with varying densities (2460 kg/m^3 ≤ ρ_p ≤ 6050 kg/m^3).

Table 2.1 Studies of local flow structure in cylindrical (Van Velzen et al., 1974; He et al., 1994) and conical (Olazar et al., 1995; 1998; 2001; San Jose et al., 1998a; 1998b) spouted beds

Author	Material Properties	Parameters					Observations in Spout	Observations in Annulus
		γ (°)	D_c (mm)	D_i (mm)	H_b (mm)	U_o/U_{ms}		
Van Velzen et al. (1974)	Glass; 0.82, 1.06 mm; 2600 kg/m^3	31	125	40	150,300	NA	Particle maximum velocity decreases as static bed height increases	Particle velocity slightly increases with static bed height
He et al. (1994)	Glass; 1.4 mm; 2500 kg/m^3	60	152	19	325	1.1,1.2, 1.3	Particle velocity increases with increasing spouting gas flowrate	No significant effect of spouting gas flowrate on particle velocity
Olazar et al. (1995)	Glass; 1, 2, 3, 4, 6, 8 mm; 2420 kg/m^3	28, 33, 36, 39, 45	360	30, 40, 50	100, 300	1.02	Particle velocity decreases with increasing axial height and gas-inlet diameter.	Not investigated
Olazar et al. (1998)	Glass; 3, 4, 5 mm; 2420 kg/m^3	33, 36, 45	360	30, 40, 50	180	1	Particle velocity increases with increasing cone angle.	No significant effect of conical angle on particle velocity
San Jose et al. (1998a)	Glass; 3, 4, 5 mm; 2420 kg/m^3	33, 36, 45	360	40	180	1	Solids hold-up increases with axial height and cone angle	Axial height has no significant effect on solids hold-up
San Jose et al. (1998b)	Glass; 4 mm; 2420 kg/m^3	33, 36, 45	360	40	180	1	Solid circulation increases with increasing cone angle	Not investigated
Olazar et al. (2001)	Glass; 4 mm; 2420 kg/m^3	30, 45, 60, 120, 180	360	30	200	1.02	$U_{p,45°} > U_{p,30°} > U_{p,60°} > U_{p,120°} > U_{p,180°}$	No significant effect of cone angle on particle velocity

Table 2.2 Studies of local flow structure in cylindrical (Santos et al., 2012; Ali et al., 2016; Aradhya et al., 2017) and conical (San Jose et al., 2005; 2006; Wang et al., 2009; Kulah et al., 2016) spouted beds

Author	Material Properties	Parameters					Observations in Spout	Observations in Annulus
		γ (°)	D_c (mm)	D_i (mm)	H_b (mm)	U_o/U_{ms}		
San Jose et al. (2005)	Glass, PP, EPS, PE; 3.5 mm; 65 to 2420 kg/m^3	33, 36, 45	360	30	150, 180, 230	1.02	$\varepsilon_{s,65\ kg/m^3} > \varepsilon_{s,890\ kg/m^3} > \varepsilon_{s,1030\ kg/m^3} > \varepsilon_{s,2420\ kg/m^3}$	$\varepsilon_{s,65\ kg/m^3} > \varepsilon_{s,2420\ kg/m^3} > \varepsilon_{s,890\ kg/m^3} > \varepsilon_{s,1030\ kg/m^3}$
San Jose et al. (2006)	Glass, PP, EPS, PE; 3.5 mm; 65 to 2420 kg/m^3	33, 36, 45	360	30	50, 150, 180	1.02	$W_{p,1030\ kg/m^3} > W_{p,890\ kg/m^3} > W_{p,2420\ kg/m^3} > W_{p,65\ kg/m^3}$	Particle velocity increases with decreasing particle density
Wang et al. (2009)	Glass; 1.16 mm; 2500 kg/m^3	45	450	19	396	1.04	Particle velocity decreases while solids hold-up increases with increasing axial height	Particle velocity slightly decreases with increasing axial height, while solids hold-up not affected.
Santos et al. (2012)	Glass; 2.2 mm; 2460 kg/m^3	60	119	20	120	NA	Optical probe presence decreases the fountain height	Not Investigated
Kulah et al. (2016)	Zirconia; 0.5, 1 mm; 6050 kg/m^3	30, 45, 60	150	15	100, 140	1.25	Particle velocity decreases while solids hold-up increases with increasing axial height. Solid circulation is higher in low conical angles.	No significant effect of any parameter on particle velocity, solids hold-up and flux
Ali et al. (2016)	Glass, Steel; 1.1, 2.2 mm; 2450, 7400 kg/m^3	60	76, 152	9.5, 19	160, 320	1.04, 1.08	Using dimensionless groups is not sufficient to maintain the similarity in local solids hold-up for a scale-up process in spouted beds.	
Aradhya et al. (2017)	Glass, Steel; 1.1, 2.2 mm; 2450, 7400 kg/ kg/m^3	60	76, 152	9.5, 19	160, 320	1.04, 1.08	There is non-similarity in local solids hold-up when the dimensionless groups of two distinct cases are matched.	

Spout-fluid beds compared to spouted beds, have more vigorous flow especially in the annulus, caused by auxiliary fluidizing gas flow, benefitting it with higher solid circulation and mixing. As tabulated in **Table 2.3**, there are few studies conducted in spout-fluid beds in literature. Sutanto et al. (1985) published the pioneering work on investigation of fluidizing gas distribution in cylindrical spout-fluid beds and its influence on particle circulation by using particle tracking method. They found that different jet shapes formed with various auxiliary gas flows. In addition, the solid circulation was higher for beds with higher static bed heights, however the effect was opposite for low static bed heights. Berruti et al. (1988) used draft tube in the half-cylindrical spout-fluid bed and studied the particle circulation. Draft tube presence showed a more homogeneous particle distribution. Pianarosa et al. (2000), on the other hand, used optical probe system to measure particle velocity and solids hold-up in cylindrical spout-fluid bed. They observed that the solids hold-up in spout region increased with fluidizing gas and was almost independent of particle size. Nagashima et al. (2015) used particle image velocimetry to measure particle velocity in cylindrical spout-fluid bed and accentuated that fluidizing gas presence increased the particle velocity in both spout and annulus regions. Although mentioned studies examined the effect of fluidizing gas in various conditions, all of the particles used were low-density particles (ρ_p < 2500 kg/m^3), revealing that local flow structure investigation in spout-fluid beds operating with high-density particles is also absent. Therefore, the effect of fluidizing gas on particle velocity, solids hold-up and particle flux was studied in this work.

Table 2.3 Studies of local flow structure in cylindrical spout-fluid beds

Author	Material Properties	Operational Conditions					Observations in Spout	Observations in Annulus
		γ (°)	D_c (mm)	D_i (mm)	H_b (mm)	U_o/U_{ms}		
Sutanto et al. (1985)	Millet, EPS, PE; 2.9, 3.9 mm; 930 kg/m^3, 1140 kg/m^3	60	152	19, 25	300,450,600	NA	Solid circulation increases with fluidizing gas for higher bed heights while it decreases for lower static bed heights	Particle velocity increases with increasing fluidizing gas
Berruti et al. (1988)	Silica Sand; 1.02 mm; 1540 kg/m^3	60	200	27	NA	0.28, 1.01	Solid circulation increases with increasing spouting gas velocity and fluidizing gas flow	Not investigated
Pianarosa et al. (2000)	Glass; 1.3, 1.8, 2.5 mm; 2500 kg/m^3	60	152	60	280	1.2	Particle velocity decreases and solids hold-up increases as fluidizing gas flow increases	Particle velocity decrease is more significant for bigger particle size
Nagashima et al. (2015)	Glass, Sand; 0.9, 1.4 mm; 2500 kg/m^3	60	100	12	150,200	NA	Particle velocity increases as fluidizing gas increases	Particle velocity increases as fluidizing gas increases

CHAPTER 3

EXPERIMENTAL SETUP

3.1 Conical Spouted and Spout-Fluid Beds

The experiments for local flow structure investigation were carried out in small and large scale conical spouted beds. The small-scale conical spouted beds are illustrated in **Figure 3.1**. They are called small-scale because their conical section height (H_c) and cylindrical diameter (D_c) are relatively smaller than the beds designed and constructed afterwards. These small-scale beds were also used in previous studies (Sarı et al. 2012, Kulah et al. 2016). The small-scale beds are made of polyoxymethylene (also known as Delrin) which is a thermoplastic easily enduring the continuous hard impacts caused by particles without significant erosion. These systems are composed of 2 parts; bottom conical bed and upper transparent cylinder.

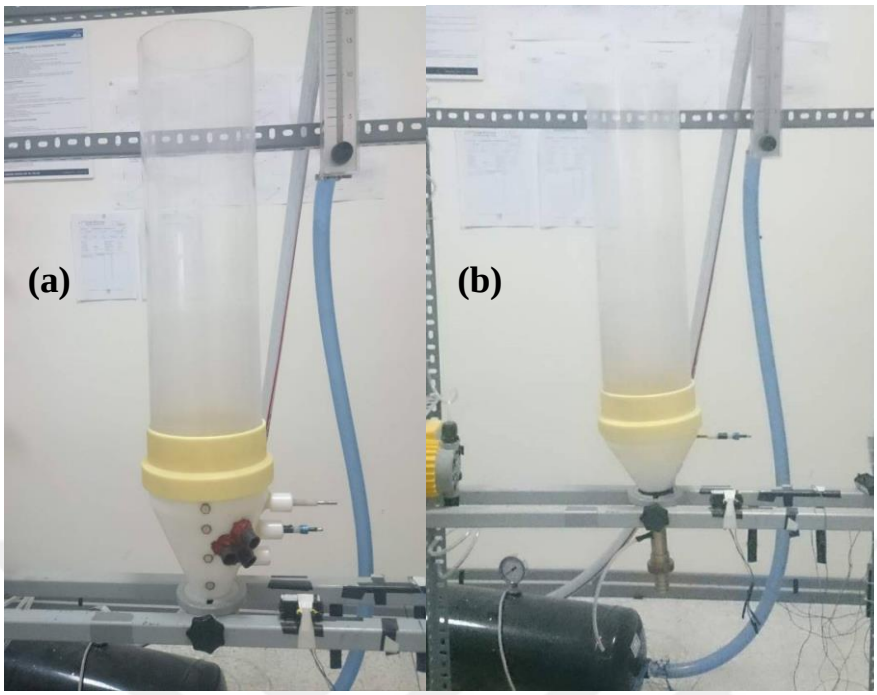

Figure 3.1 Photographs of (a) 45º and (b) 60º conical beds

Since the small-scale beds are made of thermoplastic, it is inevitable that the beds are exposed to static electricity during the operation. It causes particles to stick to the lateral wall. Therefore the entire setup was grounded during each experiment. To avoid this phenomenon, the large-scale beds, shown in **Figure 3.2**, are made of carbon steel. By this way, the static electricity influence was removed. Furthermore its resistance against erosion and hard impacts provided better performance. A schematic view of conical spouted bed and geometric parameters of the beds are presented in **Figure 3.3 and Table 3.1**, respectively.

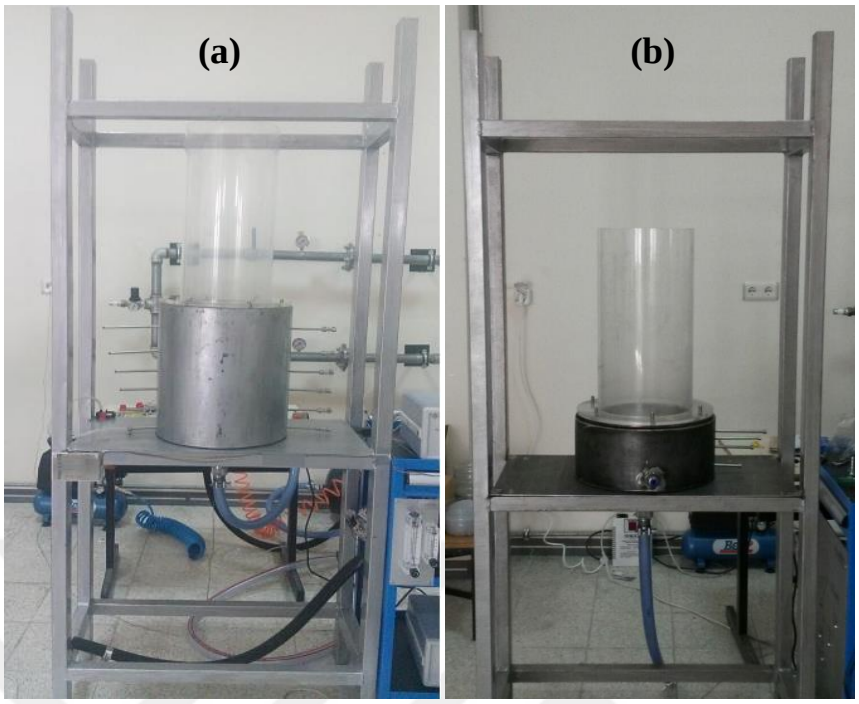

Figure 3.2 Photographs of (a) 31º and (b) 66º conical beds

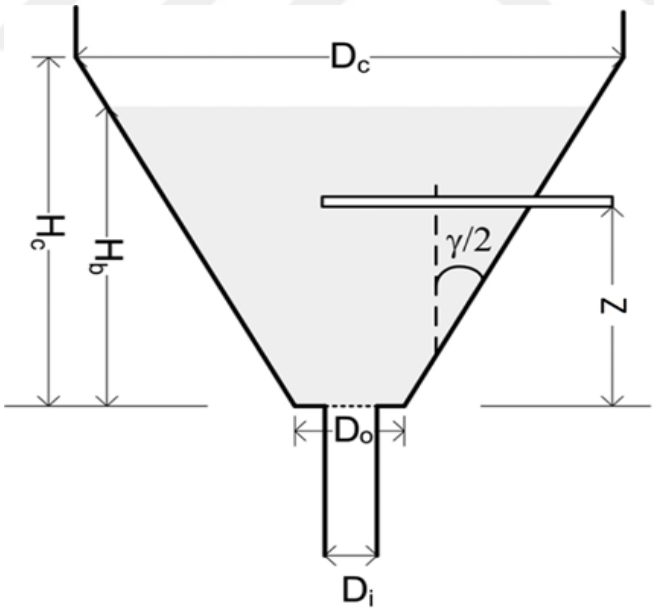

Figure 3.3 Geometric illustration of conical-spouted beds (Kulah et al., 2016)

Table 3.1 Geometric dimensions of the conical spouted beds

Parameters	**Small Scale**		**Large Scale**	
γ (°)	**45º**	**60º**	**31º**	**66º**
D_c (mm)	150	150	250	250
D_o (mm)	25	25	40	40
D_i (mm)	12 , 15	12 , 15	15	15
H_c (mm)	151	108	391	155
H_b (mm)	140	100	235	144
$z_{1,2,3}$ (mm)	42, 82, 120	50	64, 128, 185	50, 72, 100

Large-scale systems additionally have bottom fluidizing cylinder surrounding the conical base and a cylindrical plexiglass (polymethylmethacrylate) column on top, which provides visual observation of particle movement. This fluidizing cylinder is for introduction of the fluidizing gas to the system, acting the role of “wind box”, enabling these systems to be used also as spout-fluid beds. For this purpose, the conical section of beds were uniformly drilled with 1 mm diameter holes for the fluidizing gas to flow through lateral side of conical section, as illustrated in **Figure 3.4**. Based on the design criteria of distributor plate that is used in fluidized bed systems and previous experiences in spout-fluid bed operations, the open area on the lateral surface was chosen as 0.4%. With this open area ratio, the fluidizing gas was evenly dispersed inside the bed and the pressure drop arising from the holes was small.

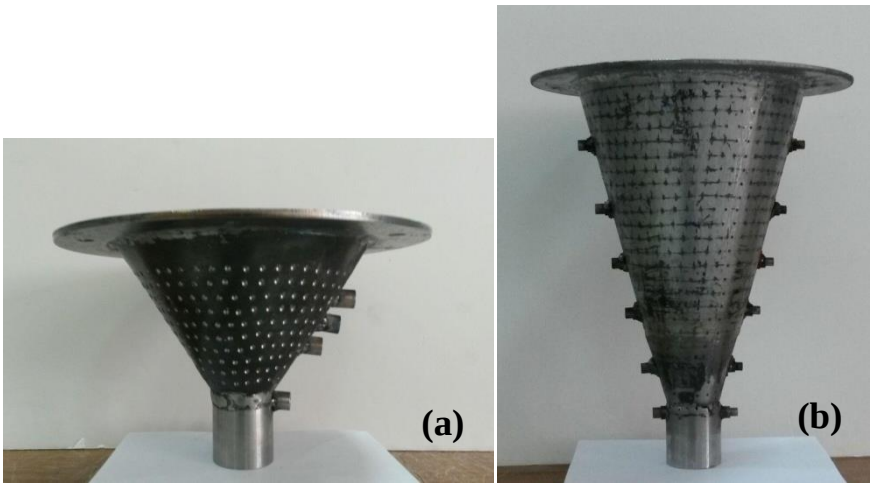

Figure 3.4 Photographs of conical spout-fluid beds with their holes on the lateral surfaces (a) 66° conical angle (b) 31° conical angle

Compressed air at ambient conditions was introduced to the systems as the spouting gas and fluidizing gas. It was supplied from a screw type of compressor operating at 8 bar and maximum flow rate of 3 m^3/min. Two air tanks of maximum 30 L volumetric capacity were positioned in series between the main air line and the system in order to eliminate the possible fluctuations of the air flow rate. Two mass flow controllers (Alicat MCR- 1500SLPM-D/5M), having maximum capacity of 1.5 m^3/min, were utilized to adjust the air flow rate and send in a controlled manner. The entire experimental setup is sketched in **Figure 3.5**.

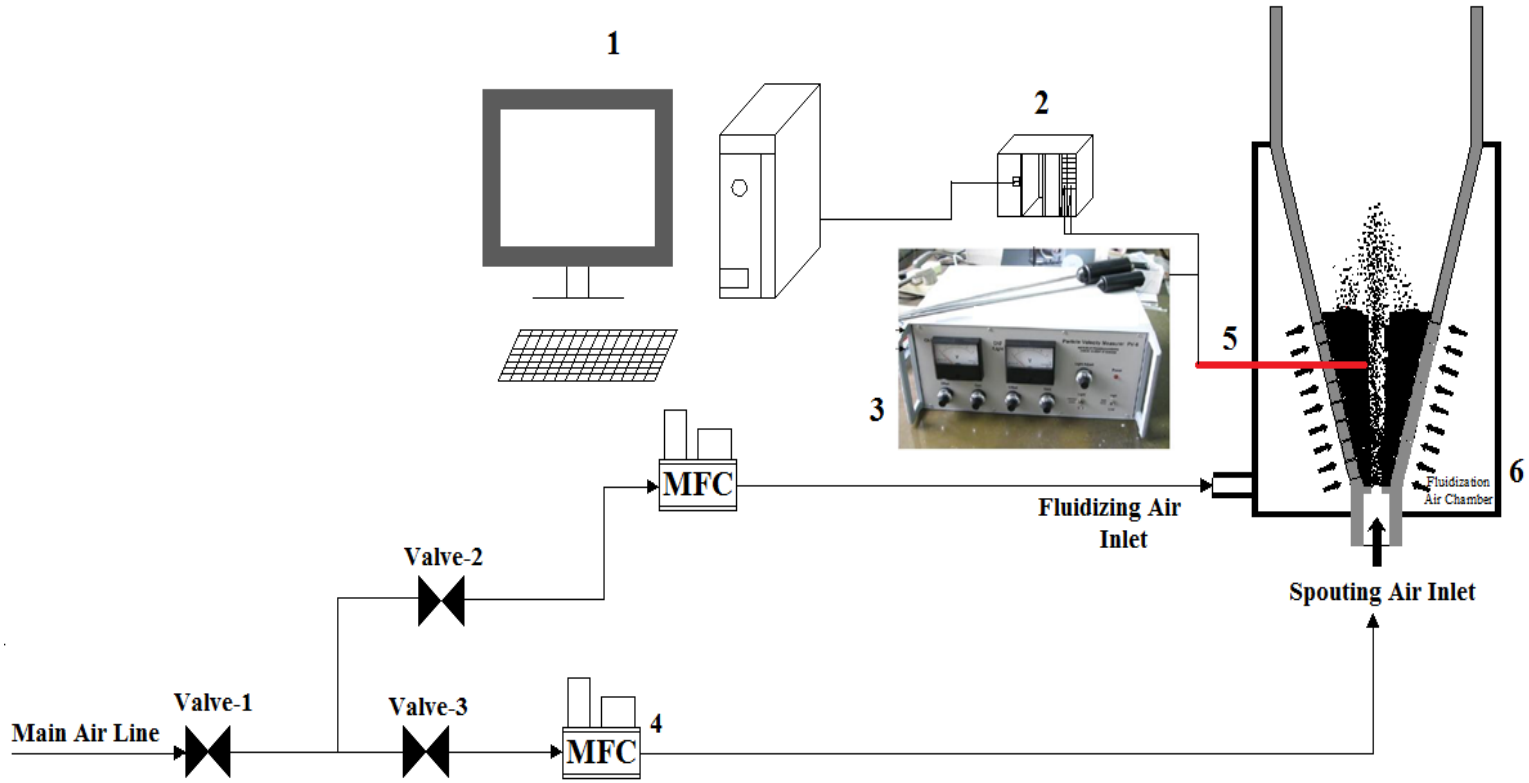

Figure 3.5 Experimental Set-up: (1) Computer, (2) Data Acquisition Card, (3) PV-6 System, (4) Mass Flow Controller, (5) Optical probe, (6) Spout-Fluid Bed

In this study, glass beads, alumina (zirconia toughened) and yttria-stabilized zirconia (YSZ) particles, as shown in **Figure 3.6**, were used. The properties of these particles are given in **Table 3.2**. All particles are spherical and have 1 mm diameter. These particles are especially chosen as their densities represent both light and heavy particles. Glass beads is regarded as light particles while alumina and zirconia are regarded as heavy particles. The loosely packed solids hold-up, $\varepsilon_{s,0}$, was calculated by a volumetric calculation in graduated cylinder.

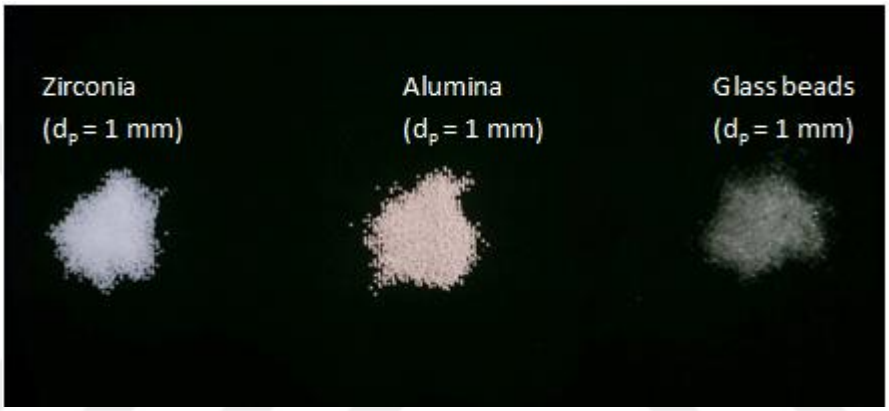

Figure 3.6 Photograph of the particles

Table 3.2 Properties of the particles used in the experiments

Particles	d_p (mm)	φ	ρ_p (kg/m^3)	$\varepsilon_{s,0}$
Glass Beads	1	1	2460	0.63
Alumina (zirconia toughened)	1	≥ 0.95	3700	0.60
Zirconia	1	≥ 0.95	6050	0.61

3.2 Optical probe measurement system

Particle velocity, solids hold-up and particle flux are the main parameters giving the information about the local flow structure in conical spouted beds. For the measurement of these quantities, fiber optical probe system, which is illustrated in **Figure 3.7**, was used in this study. The Particle Velocity Analyzer (PV-6) system is designed by Fluidization Research Center of the University of British Colombia (Canada) and manufactured in China by the Institute of Process Engineering. It consists of optical probes and a data collection box.

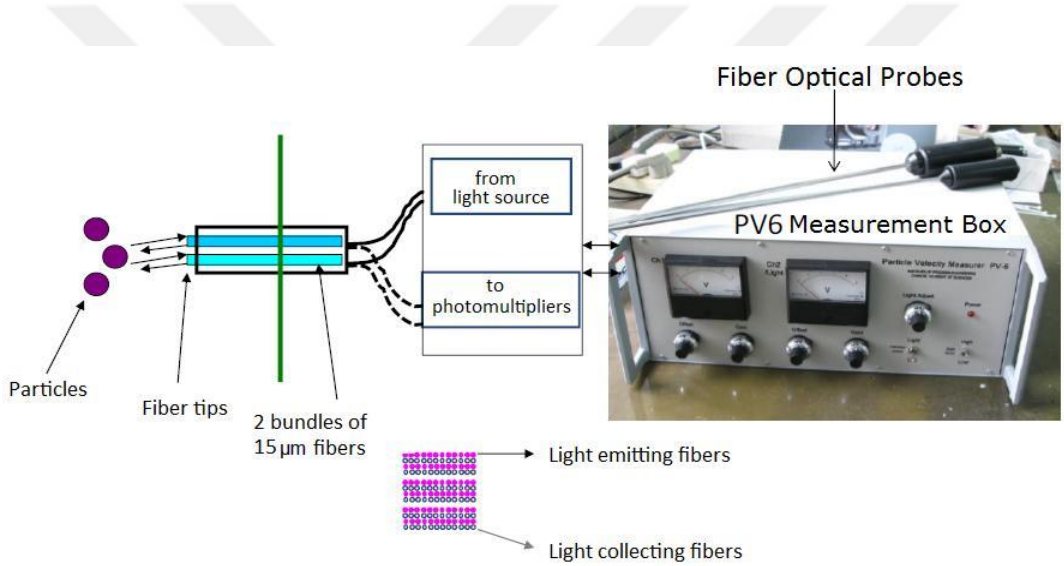

Figure 3.7 PV-6 Particle velocity and solids hold-up measurement system

As it can be seen in the figure, the probes have two bundles of fibers inside. These bundles contain consecutively sorted light emitting and light collecting fibers. The optical probe can be inserted at any axial height and can measure particle velocity and solids hold-up simultaneously.

The working principle of optical probe is based on luminary phenomena. As illustrated in **Figure 3.8**, the light is emitted from the fiber tips and when it arrives to

particle surface, it is reflected back to the probe and collected by the light collecting fibers. Collected light is sent to two photomultipliers belong to two distinct channels, providing two different signals. After that, the signals are loaded into computer as raw data, by virtue of high-speed data acquisition card. During this process, a software named LabVIEW® from National Instruments is used. Obtained raw data is processed by a MATLAB code which was developed by Kirbas (2004) and lastly, particle velocity, solids hold-up and particle flux are calculated. The working algorithm behind the MATLAB code is illustrated in **Figures 3.9 and 3.10**.

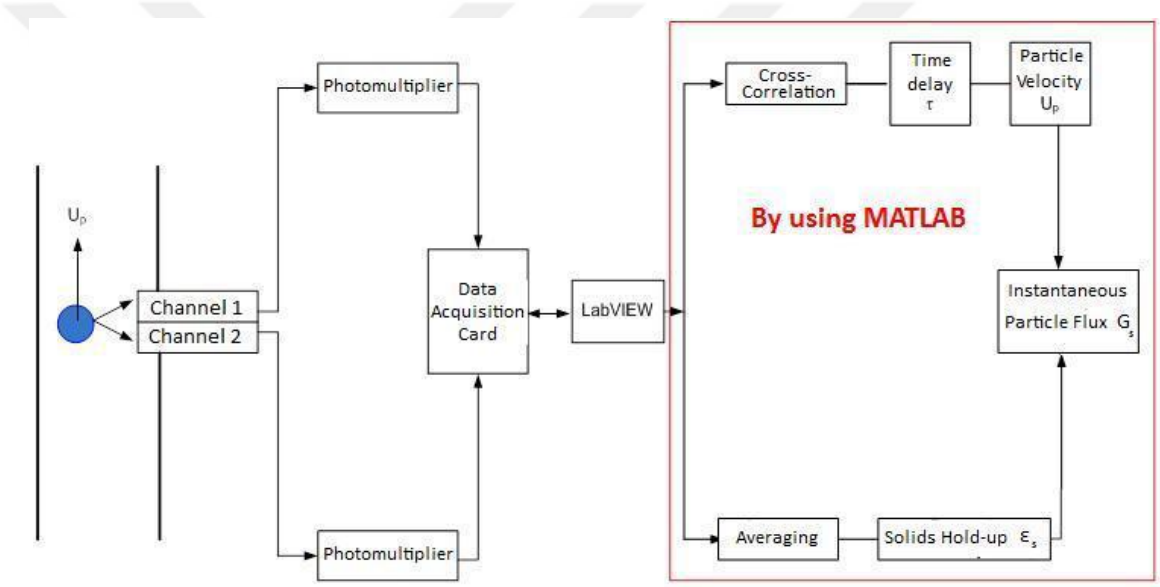

Figure 3.8 Particle velocity, solids hold-up and particle flux calculation steps

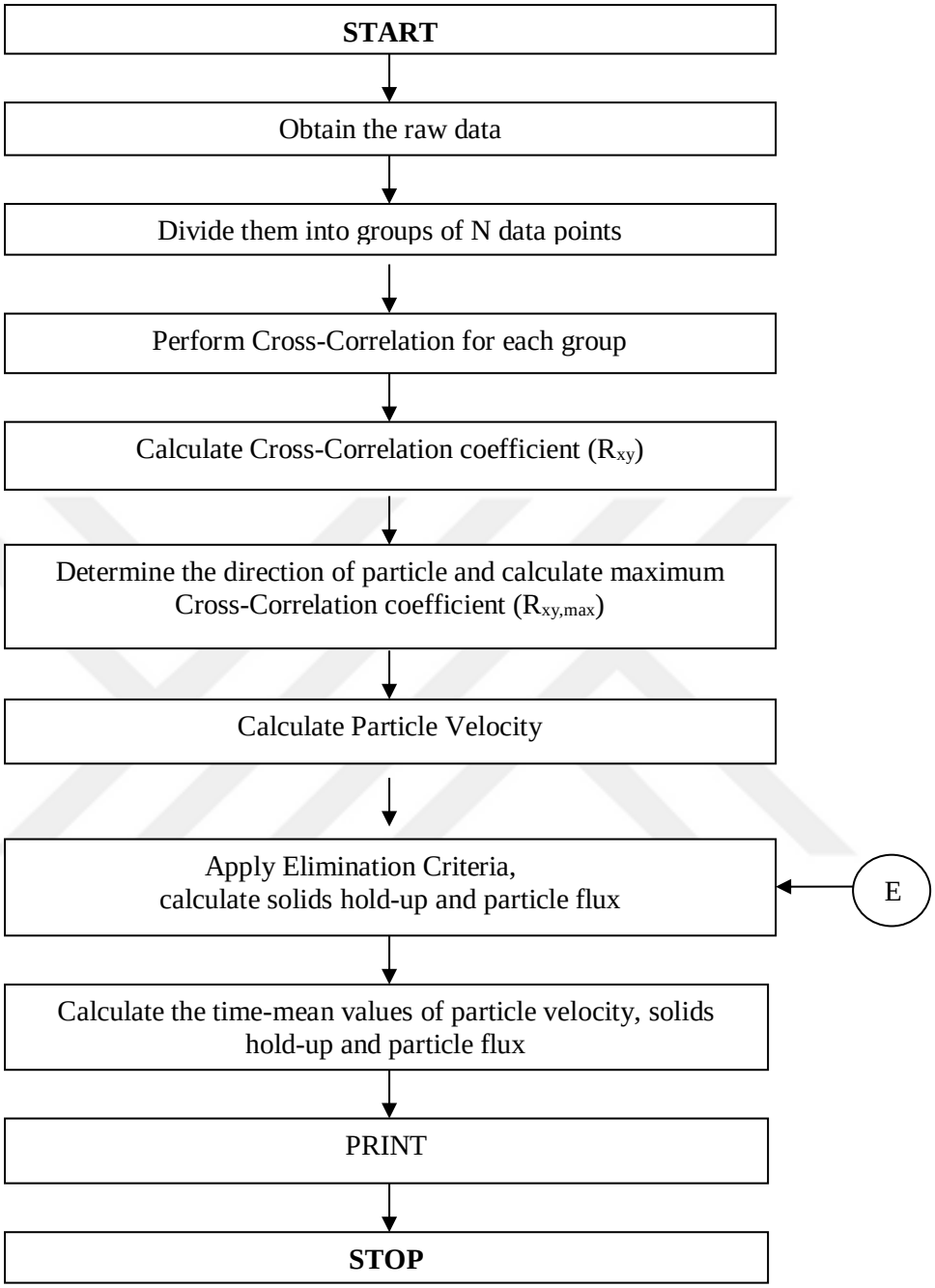

Figure 3.9 Algorithm of the main code to calculate particle velocity, solids hold-up and particle flux (Kirbas, 2004)

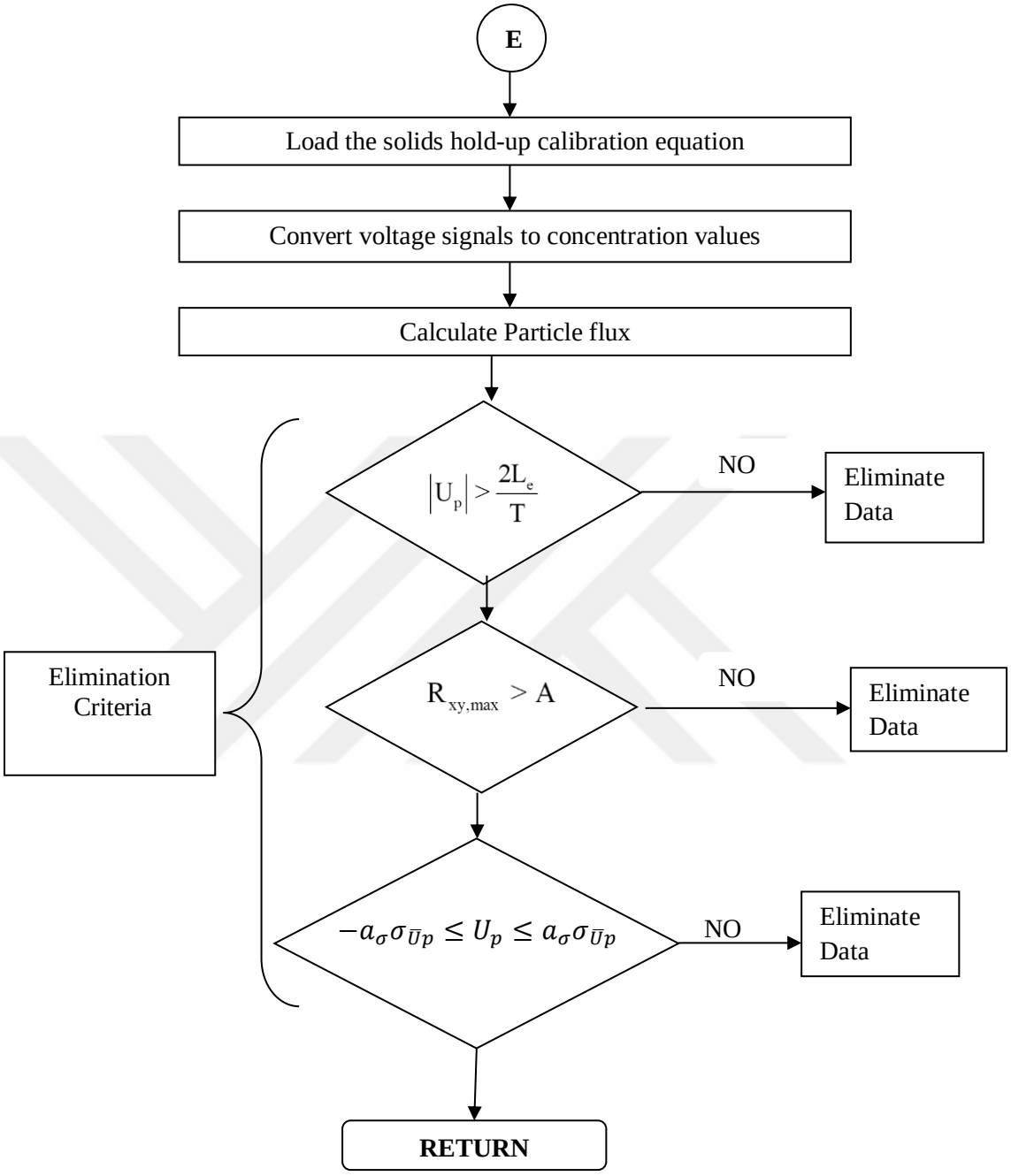

Figure 3.10 Algorithm of the sub code to run elimination criteria for calculation of solids hold-up and particle flux (Kirbas, 2004)

The velocity of a particle is calculated by the relation between the time and the distance the particle travels through the channels of the probe. When a particle passes in front of the channels of the optical probe, very similar two signals are obtained with a difference of time delay, τ. Time delay can be calculated by cross-correlation analysis using the MATLAB code, as shown in **Figure 3.11**. To calculate particle velocity, the effective distance (L_e), a parameter which needs to be determined during optical probe calibration, must be known. The particle velocity is then calculated by using **Eq. 3.1**.

$$U_p = \frac{L_e}{\tau} \tag{3.1}$$

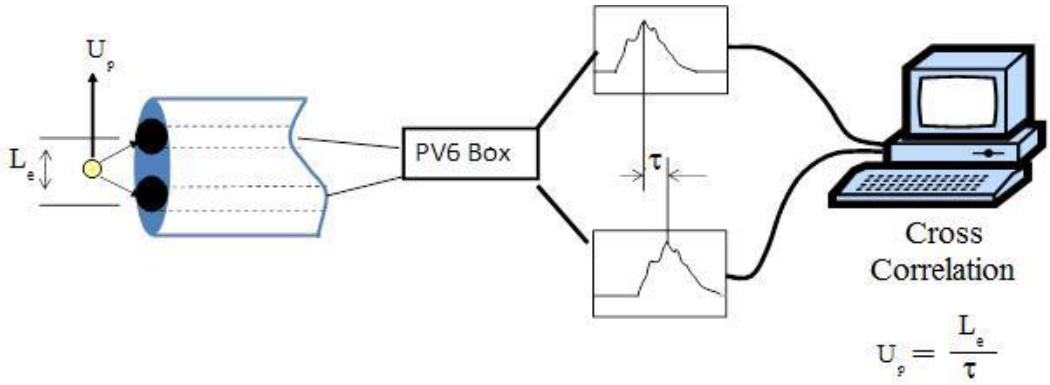

Figure 3.11 PV-6 particle velocity measurement method

Cross-correlation method is a statistical analysis method and expressed by cross-correlation functions. They are used to measure the similarity between two different data sets. This similarity is based on the time delay from the obtained data. Cross-correlation function, ϕ_{I1I2}, can be calculated by **Eq. 3.2**.

$$\Phi_{I_1 I_2}(\tau) = \lim_{T\to\infty} \frac{1}{T} \int_0^T I_1(t) I_2(t+\tau) dt \tag{3.2}$$

where $I_1(t)$ and $I_2(t+\tau)$ represent the voltage signals from two channels, that is obtained in time period of T while τ represents the time delay between $I_1(t)$ and $I_2(t+\tau)$ signals. In this study, T period is limited by sampling time of the optical probe. As a degree of correlativity between the signals, cross-correlation coefficient, R_{xy}, is used which is defined as follows:

$$R_{xy}(k) = \frac{C_{xy}(k)}{\sigma_x \sigma_y} \tag{3.3}$$

In **Eq. 3.3**, $C_{xy}(k)$ represents the cross-covariance function which examines the effect of change between two variables, σ_x and σ_y are the variance of obtained data from first and second channel, respectively. The correlation coefficient varies between 0 and 1. In a real system, two complicated signals are obtained. An example of signals obtained in 14.6 milliseconds period by two fiber bundles of optical probe is illustrated in **Figure 3.12**. After the signals are cross-correlated, the cross correlation coefficient is calculated and plotted with respect to the time delay between the signals of two channels. Here, τ represents the time delay at which the maximum cross-correlation coefficient was calculated. This value corresponds to average time that the particles pass between the two bundles of optical probe (Kulah et al., 2016).

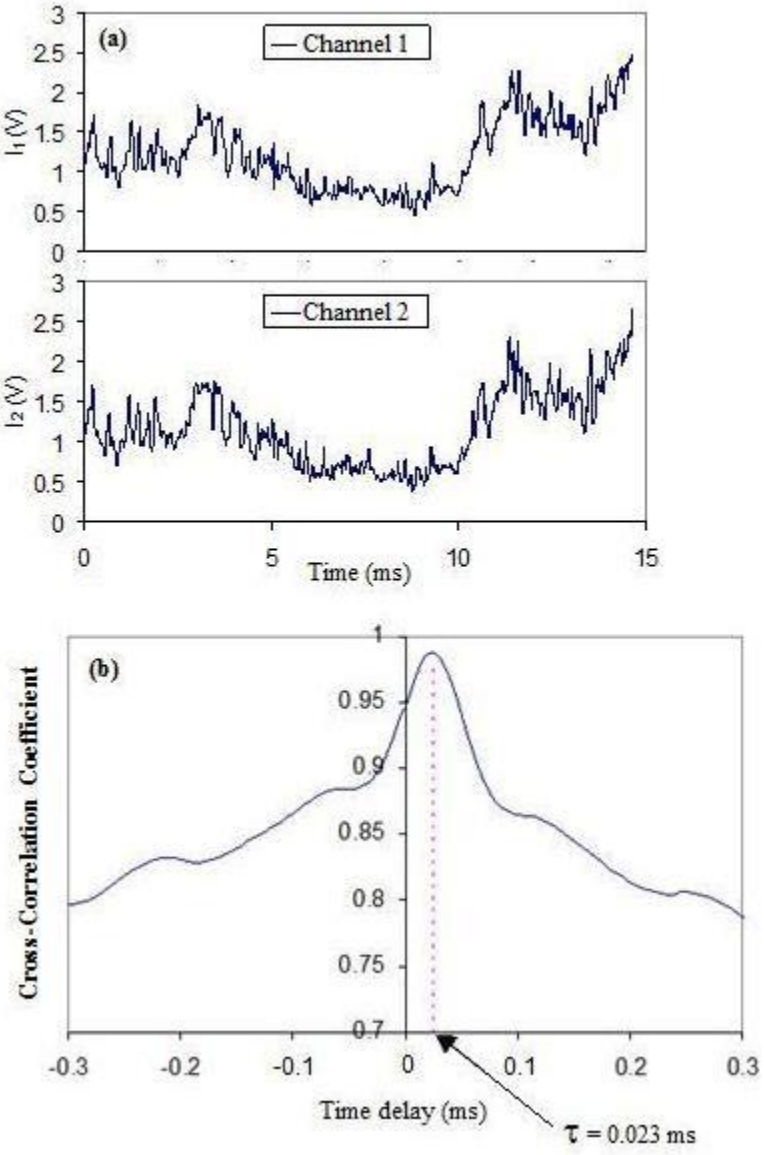

Figure 3.12 (a) Measured voltage signals in 14.6 ms time period, (b) Plot of cross-correlation coefficient vs. time delay between the signals (Sarı et al., 2011)

In addition to time delay, the effective distance, L_e, between two channels of optical probe must be known. The effective distance depends on particle properties, hence should be precisely calculated. Determination of effective distance is called ***"the calibration of optical probe for particle velocity"***. Here, the important thing to

mention is that the effective distance may not always be equal to geometrical distance between the two channels.

3.2.1 Calibration of optical probe for particle velocity and solids hold-up

The experimental setup system of optical probe for particle velocity calibration is illustrated in **Figure 3.13**. To eliminate the influence of surrounding light, the setup system is covered and measurement box was closed by a black cardboard. Also, the optical probe is passed through the cardboard to fix its location such a way that the channels are perpendicular to each other.

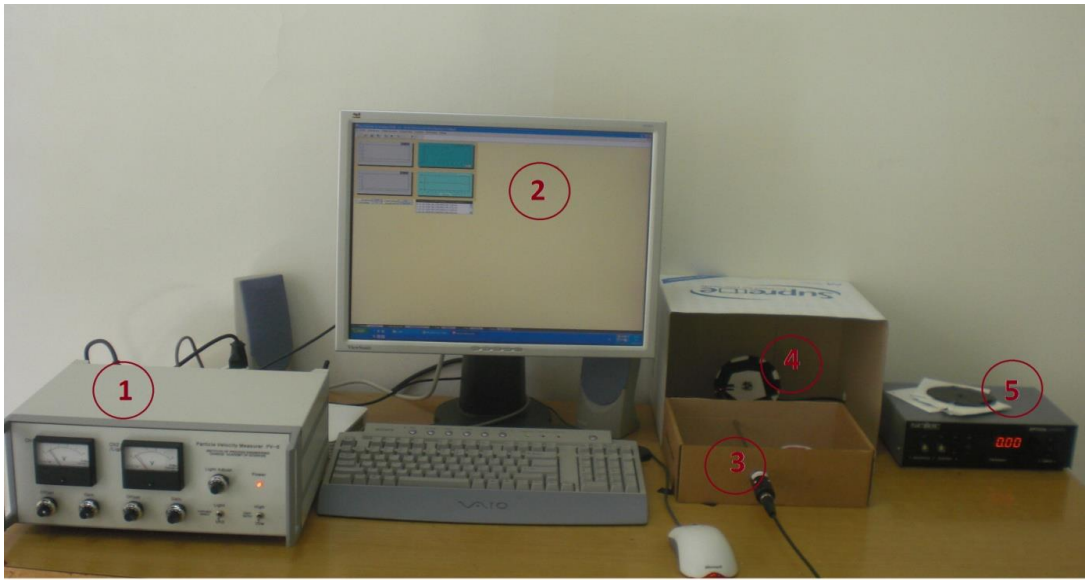

Figure 3.13 Experimental setup of optical probe for calibration of particle velocity measurements (1: PV-6 System, 2: Particle velocity analysis program, 3: Optical probe, 4: Chopper disc, 5: Optical chopper device)

In **Figure 3.14**, the chopper discs that are used in the calibration are illustrated. Chopper discs of *a*, *b*, *c* and *d* are from Edmund Optics Company and special design choppers for this calibration method while chopper discs of *e*, *f*, and *g* are that 1 mm diameter of glass, alumina and zirconia particles are adhered onto, respectively. First

four chopper discs are adhered onto a white paper. In this way, the particle movement in front of the probe tip can be simulated with frequent high signal peaks.

Figure 3.14 Chopper discs for velocity calibration, (a, b, c, d : Various indentation numbers of discs, e: Chopper disc with 1 mm glass beads, f: Chopper disc with 1 mm alumina, g: Chopper disc with 1 mm zirconia)

Each disc was run with various angular velocities. The angular velocity of disc is calculated by the **Eq. 3.4**.

$$S_d = 2\pi r_d f_d \tag{3.4}$$

Here, S_d, r_d, and f_d represent the angular velocity of chopper disc, the distance of optical probe tip to chopper disc center, and rotation frequency of chopper discs, respectively. For each angular velocity, time delay τ was calculated by MATLAB code. Then the effective distance was calculated and tabulated in **Table 3.3** and **Table 3.4**. In this study, two different optical probes were used and their effective distances were calculated as 2.11 mm and 2.56 mm, respectively.

Table 3.3 Averaged effective distances of chopper discs and their standard deviations (Probe #1)

Chopper Disc	**Effective distance, L_e (mm)**	**Standard Deviation**
a	2.105	0.1959
b	2.101	0.0417
c	2.119	0.0196
d	2.105	0.0945
e (Glass) d_p = 1 mm	2.111	0.0383
f (Alumina) d_p = 1 mm	2.116	0.0143
g (Zirconia) d_p = 1 mm	2.112	0.0243

Table 3.4 Averaged effective distances of chopper discs and their standard deviations (Probe #2)

Chopper Disc	**Effective distance, L_e (mm)**	**Standard Deviation**
a	2.52	0.095
b	2.55	0.069
e (Glass) d_p = 1 mm	2.56	0.102
f (Alumina) d_p = 1 mm	2.56	0.101
g (Zirconia) dp = 1 mm	2.56	0.091

The optical probe has also the ability to measure the solids hold-up. Solids hold-up is a dimensionless value indicating the particle concentration in the system. It is the ratio of solid volume over the total volume, therefore it is the opposite of void fraction, the voidage. Optical probe measures the solids hold-up by using a relationship between voltage signals that optical probe collects and particle concentration in the measurement area. The determination of this relationship is called ***"the calibration of optical probe for particle concentration"***. In literature, various calibration methods are presented. One of them is solid-solid mixture technique used by Kirbas (2004) and Wang (2006). This technique involves the mixtures of different mixtures of particles with black and standard color. In Kirbas (2004), different mixtures of FCC particles and coking coal were prepared. Coal was chosen because of its black color which has the ability to absorb the light.

In this study, a similar calibration setup to the one used in Kirbas (2004), shown in **Figure 3.15**, was used. There are three parts of the setup: First part has 30 mm inner diameter pipe to contain the particles by the upper valve. When the upper valve is opened, the particles move to the second part with 12 mm inner diameter pipe where the optical probe is inserted. The third part is the black vessel that the particles are

collected. The calibration setup was painted to black in order to minimize the light effects from surrounding lights. All calibration measurements are done in LabVIEW software with 100 kHz sampling frequency and 10 seconds of sampling time.

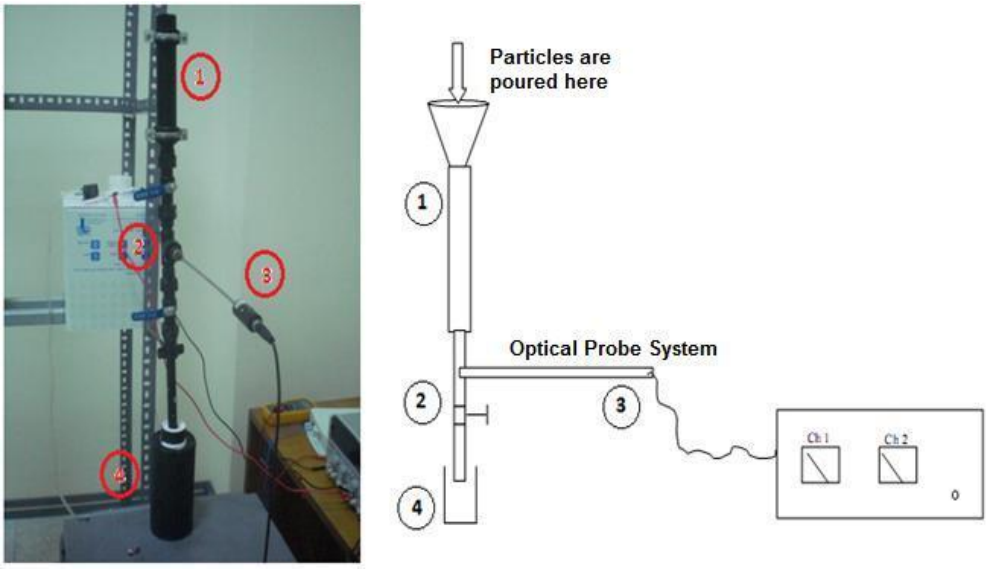

Figure 3.15 Calibration setup used for particle concentration measurement: (1) 30 mm inner diameter vessel, (2) 12 mm inner diameter pipe, (3) optical probe, (4) Particle collecting vessel

In this study, the same solid-solid mixture technique was used. Some portions of particles were painted to black, thus the black particles absorb the light and optical probe collects low voltage signals which correspond to void. On the other hand, original particles reflect the light and optical probe collects high voltage signals which correspond to particle detection. Different mixtures of particles were prepared based on their weight percentage to simulate every condition in the real bed system. **Figure 3.16** shows alumina mixtures with different black particle concentration. The mixtures of all particles were prepared as follows:

- Glass : 0%, 25%, 50%, 75%, 100%
- Alumina : 0%, 25%, 50%, 75%, 100%
- Zirconia : 0%, 10%, 30%, 50%, 70%, 90%, 100%

Figure 3.16 Alumina mixtures (a: 0%, b: 25%, c: 50%, d: 75%, e: 100%)

Particle concentration calibration has two steps. In the first step, signal measurements are taken for 0% and 100% black mixtures when they are in loosely packed state. This is for determining the minimum and maximum voltage signals. In the second stage, the mixtures are poured through conical mouth, and flow is provided. By adjusting the lower valve, particles flow down slowly and signal measurements are

taken. This is for simulating the flow regime in loosely packed state. The inner diameter of part two is smaller for providing a slow particle flow. Obtained voltage measurements are averaged and plotted in **Figure 3.17** for each particle. The figure shows that there is a linear relationship between the magnitude of voltage signals and particle concentration.

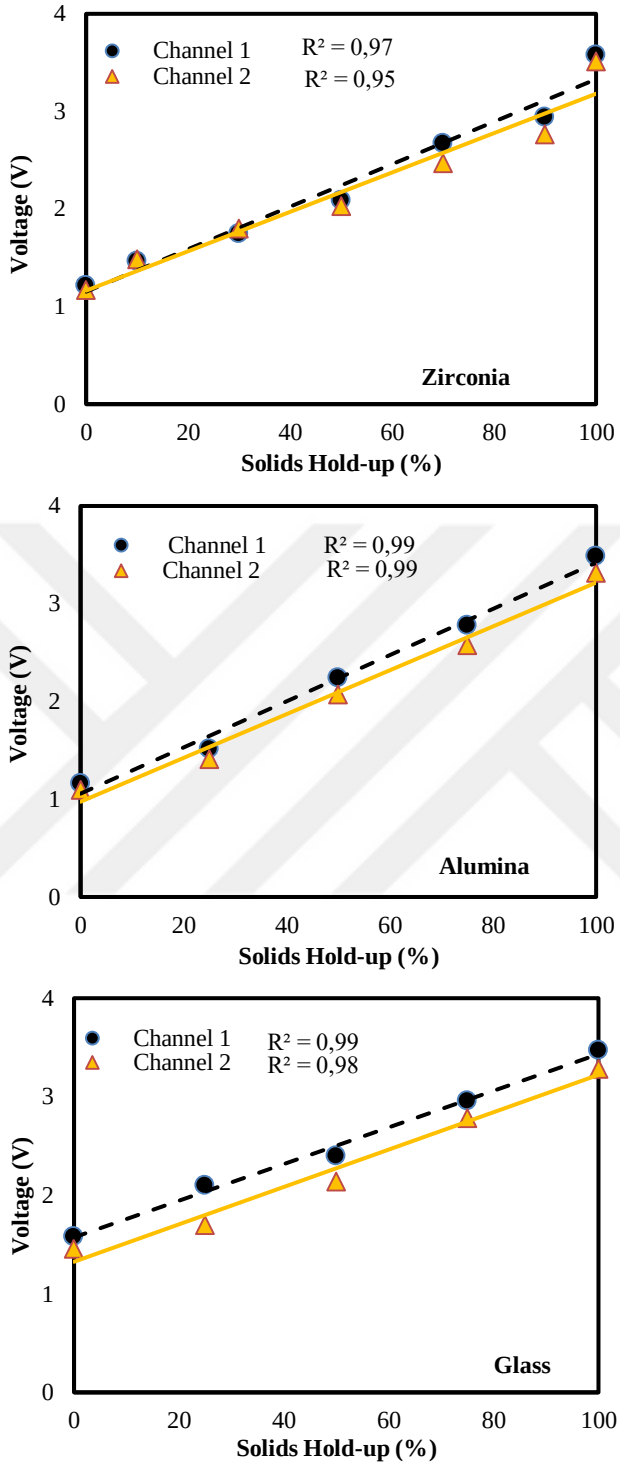

Figure 3.17 Correlated relation between the solids hold-up and the voltage for all particles (L_e = 2.56 mm)

In Wang's study (2006), this linear relationship is validated and expressed as follows:

$$V = X_b \frac{V_b}{\varepsilon_{s,0}} + X_c \frac{V_c}{\varepsilon_{s,0}} \tag{3.5}$$

where V corresponds to measured voltage signal, X_b corresponds to volume fraction of the original particles, $\varepsilon_{s,0}$ is the loosely packed solids hold-up value of particles, V_b is the corresponding voltage of original particles at the loosely packed state, while X_c and V_c are the same terms for black particles.

To define a mass fraction term Y, for original particles in the mixture, corresponding volume fractions can be expressed by **Eq. 3.6 and 3.7**.

$$X_b = Y\varepsilon_{s,0} \tag{3.6}$$

$$X_c = (1 - Y)\,\varepsilon_{s,0} \tag{3.7}$$

From the equations above, the following expressions can be obtained,

$$V = YV_b + (1 - Y)V_c \tag{3.8}$$

$$\frac{V}{V_b} = Y + (1 - Y)\frac{V_c}{V_b} \tag{3.9}$$

Since there is no painted particle in experimental system, the volume fraction of original particles X_b, is directly equal to solids hold-up $\varepsilon_{s,0}$, leading to **Eq. 3.10**. V_b and V_c values correspond to voltage signals of loosely packed particle mixtures of 0% and 100% black, respectively. Before each experiment, V_b and V_c values are measured in the calibration setup shown in **Figure 3.15**. By using the $\varepsilon_{s,0}$ and voltage signals of minimum V_c and maximum V_b, local solids hold-up value can be calculated.

$$\varepsilon_s = \varepsilon_{s,0} \frac{V - V_c}{V_b - V_c} \tag{3.10}$$

3.2.2 Data Processing

The raw data obtained by optical probe system in the experiments were processed by MATLAB code, whose algorithm is shown in **Figure 3.9** and **Figure 3.10**, and particle velocity, solids hold-up and particle flux were calculated. Total raw data was first divided into groups of N data number, and each group was cross correlated with a resulting cross-correlation coefficient, R_{xy}. During the analysis of each group, it was firstly assumed that the particles are moving in upward direction and calculated R_{xy} is called as $R_{xy,up}$. Then particles were assumed to be moving in downwards direction and $R_{xy,down}$ was calculated. These coefficients were compared and code assigned the greater coefficient as maximum coefficient, $R_{xy,max}$ and determined the direction of particles (Sarı et al. 2011).

Particles in spouted beds may move in opposite direction or angular direction due to the flow structure which significantly affects the optical probe measurements. Because any particle passing in front of one channel of optical probe may not be detected by the second channel. Such cases decrease the similarity between two signals and hence a poor correlation is calculated leading to inaccurate time delay and particle velocity. Therefore it is better to eliminate low correlated data obtained in such conditions. In this context, the elimination criteria, proposed in Kirbas (2004), was applied.

1) Elimination of values in this range, $\pm\left|U_{p,min}\right| = \frac{2L_e}{T}$
2) Elimination of values for which R_{xy} > A, a certain lower limit for cross-correlation coefficient
3) Elimination of particle velocities for which is out of a limit determined by standard deviation, $-a_\sigma \sigma_{\bar{U}p} \leq U_p \leq a_\sigma \sigma_{\bar{U}p}$

First criterion was used for the limitations of the measurement system and cross-correlation. The lowest measurable absolute particle velocity depends on sampling time, *T*, used in cross-correlation. This value is equal to total data number divided by sampling frequency. For example, to make a group with 5000 data number with a

1000 Hz sampling frequency, 5 seconds must elapse. Time delay τ cannot be bigger than *T/2*. The particle velocity for this limit time delay is equal to $|U_{p,min}|$, the lowest measurable particle velocity (Sarı et al. 2011). The second criterion is about the particle movement in the bed system. According to degree of similarity, low correlated groups are eliminated, while relatively high correlated groups are included. Third criterion is about particle velocity and standard deviation. A certain interval is obtained by multiplication of standard deviation with variance interval coefficient (Kirbas, 2004). If measured particle velocity is out of this interval, it is eliminated. The variance coefficient determines the degree of tolerance for particle velocity. These values were chosen in light of the findings of Kirbas (2004).

As previously mentioned, there are two main regions in spouted beds: Spout and annulus. Since particle flow structure is different in these regions, they should be distinctly analyzed and sampling time and frequency should be chosen accordingly. Therefore, a sensitivity analysis was carried out to determine the parameters used in optical probe measurements.

3.2.3 Sensitivity Analysis

In order to catch the fast particle movement in the spout region, the measurements should be done with high sampling frequency. As for annulus region, there is no such requirement due to slow particle motion. However, sampling time should be long enough to have sufficient number of data to be analyzed. For these reasons, sampling frequency with sampling time were chosen as 100 kHz with 10 seconds and 1 kHz with 120 seconds for spout and annulus regions, respectively.

As given in **Figure 3.9 and 3.10**, the whole data was firstly divided into groups of each having N data number. Cross-correlation was applied to each group. Therefore, each group must have sufficient number of data in order to catch the characteristics of the flow. On the other hand, as N increases, the correlation quality decreases due to more number of data are tried to be correlated with each other. An optimum value of N should be found based on these limitations.

During the cross-correlation analysis, there is a parameter limiting the number of data to be shifted to catch the similarity. This parameter is called max_lag. Briefly, it determines how many data in one group that the program is allowed to shift, so that the two signals can be correlated. This shifting process is the shifting of data belonging to only one channel while the other one is fixed. In each unit step, the program shifts one data and calculates the cross-correlation coefficient. For example, two different signals are divided into groups of 4000 data. In the first unit step, the interval between 0th and 4000th data belong to two signals are investigated. The next unit step analyses the similarity between the intervals of 0-4000 data of fixed signal and 1-4001 data of shifted signal. If max_lag value is 2000, this process continues until 2000-6000 data interval of shifted signal. The same steps are applied on the other groups (4001-8000; 8001-12000 etc.). Different values of max_lag are input into the code and resulting particle velocities are illustrated in the **Figure 3.18**.

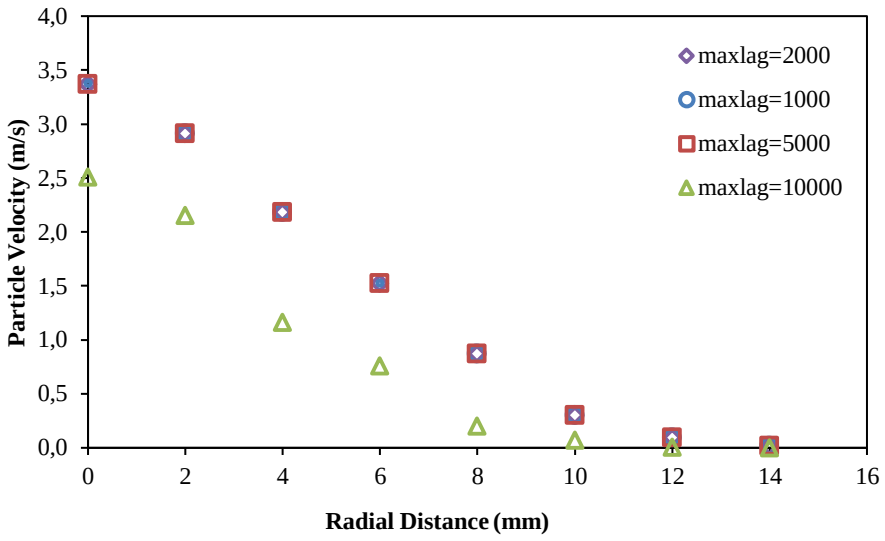

Figure 3.18 The effect of max_lag parameter on particle velocity (Zirconia, 31°, $z_2/H_b = 0.54$)

From the figure, particle velocity profiles for zirconia were found to be identical when max_lag was equal to 1000, 2000 and 5000. However, when max_lag was equal to 10000, particle velocity decreased in the spout region. This is because the program calculated a higher R_{xy} value for which max_lag = 10000, than max_lag = 2000. When the shifting data number is limited to 2000, it cannot calculate an R_{xy} for shifting any data beyond that point, which means to ignore any new maximum values of R_{xy}. This leads the program to calculate higher particle velocity, because the corresponding time delay is shorter.

Because max_lag plays the role of giving the certain point at which the maximum similarity (R_{xy_max}) is observed, its determination is very delicate. Therefore, various max_lag values were tried to observe the effect on R_{xy}. In **Figure 3.19**, the relation between max_lag and R_{xy} is illustrated. It is seen that maximum R_{xy} was calculated as 0.51 when the program is allowed to shift up to 2000 data points. In the same case, the maximum R_{xy} was calculated as 0.70 when max_lag = 10000. Wang (2006) stated that there may be more than one maximum cross-correlation coefficients. In such cases, the coefficient which gives the minimum time delay must be chosen. The max_lag value in this study is chosen as 2000 based on this statement.

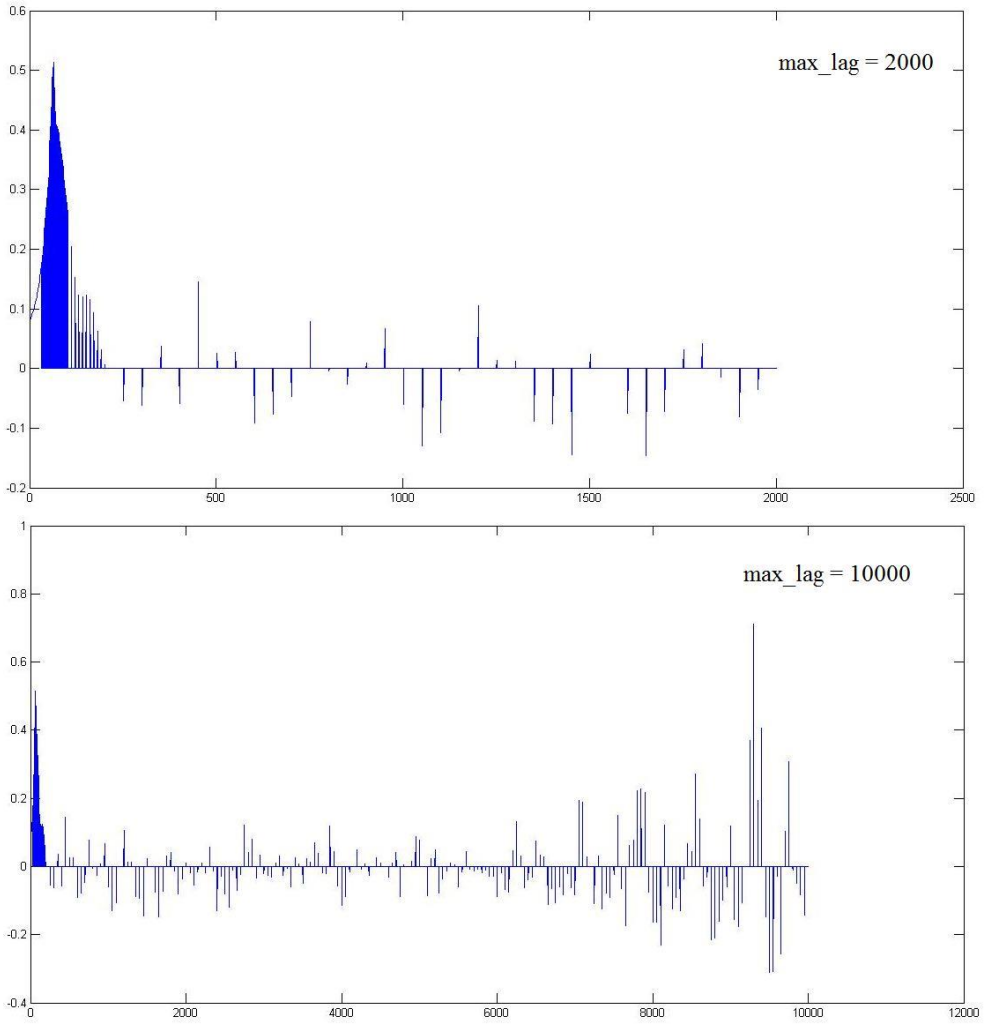

Figure 3.19 The plot of max_lag vs. R_{xy} (Alumina, 31°, $z_1/H_b = 0.27$)

The parameters decided in light of the sensitivity analyses and that were used in optical probe measurements are summarized in **Table 3.5**, for spout and annulus regions individually.

Table 3.5 Parameters used for optical probe measurements

Parameters	**Spout**	**Annulus**
Total sampled data number	1000000	120000
Sampling Frequency	100 kHz	1 kHz
Sampling Time	10 seconds	120 seconds
max_lag	2000	
Number of data in each group, N	4000	
A	0.4	
a_σ coefficient	3	

CHAPTER 4

RESULTS AND DISCUSSION

This chapter presents the results of the experimental studies undertaken within the scope of this thesis. In this thesis study, firstly, operating conditions of the conical spout and spout-fluid beds (minimum spouting and fluidizing gas flow rates) were determined. Secondly, effects of operating conditions and the bed geometry on the local flow structure are investigated. Some parts of the results obtained in this study were used in an international conference (Golshan et al., 2017). Lastly, an empirical correlation for the solids hold-up at the spout center in conical spouted beds was proposed based on the experimental outcome.

4.1 Bed Pressure Drop Measurement and Determination of Minimum Spouting Velocity

In spouted and spout-fluid bed applications, minimum spouting velocity (U_{ms}) is an operational parameter occupying an essential place. In order to have a clear observation of the influence of the bed geometry and operating parameters during the operation, a well-settled, stable flow must be present in the bed. Therefore, a certain gas velocity, named as superficial gas velocity, that is higher than minimum spouting velocity must be provided to the system. Thus, the aspects of any instability in flow such as change in fountain height, pulsative jet flow or collapse of the spout can be removed. Nevertheless, the superficial gas velocity has also an upper limit beyond which the flow regime becomes jetting. All these make the determination of the minimum spouting velocity a crucial work.

The minimum spouting velocity can be determined by measuring the bed pressure drop while ascending or descending superficial gas velocity. The minimum spouting velocity point is located around the region where the bed pressure drop becomes flat beyond the peak pressure. However to detect the exact point, visual observations must also be made. A hysteresis is observed between pressure drop measured in ascending and descending case.

In all conditions, the observed U_{ms} value during ascending is higher than descending case. This is caused by a resistance of the stationary-state particles against spouting before the onset of spouting, leading to an extra force requirement to set the particles into motion. Moreover, due to randomly packing configuration of the particles, ΔP curve in ascending case is not consistent while the descending case curve is always fixed. Therefore, in the determination of minimum spouting velocity, descending U_{ms} values were used for experiments. It is also known that the pressure drop values in ascending experiment is time dependent which results in different pressure drop values in different runs of experiments. Descending experiment, on the other hand, gives the same results with other runs of experiments because there is no effect of initial particle packing state.

In **Figure 4.1 and 4.2**, a typical change in spouting gas velocity with bed pressure drop for alumina and glass particles is illustrated. As illustrated in these figures, the bed pressure drop firstly increases with superficial gas velocity to a peak value which corresponds to the minimum internal spouting condition. Further increase in the gas velocity causes a sudden decrease in the bed pressure drop until external spouting condition is reached approximately where the pressure subsides and remains almost constant afterwards. It is observed that the pressure drop across the bed for the cases illustrated in **Figure 4.1 and 4.2** increases to approximately 4200 Pa and 5400 Pa, respectively, until the peak point is reached. After this point, since the jet is formed and onset of spouting occurs, the bed pressure drop diminishes significantly to 2200 Pa and 3000 Pa. The values of peak pressure drop and stable flat region pressure drop are different for two different cases. Because the bed pressure drop is affected

by particle density and static bed height. The minimum spouting velocities are calculated from determined gas flow rates by dividing it to the area of the inlet nozzle. Calculated minimum spouting velocities are given in **Table 4.1**. During the local flow measurements, spouting gas velocity was set to 1.25 and 1.1 times higher than the minimum spouting velocity in small and large scale systems, respectively, to ensure that experiments were performed during stable spouting operation. Before the measurements, the bed was operated for 15 minutes in order to remove the effect of unsteady flow. The sampling frequency is set to 1 kHz, and the sampling time is 10 seconds.

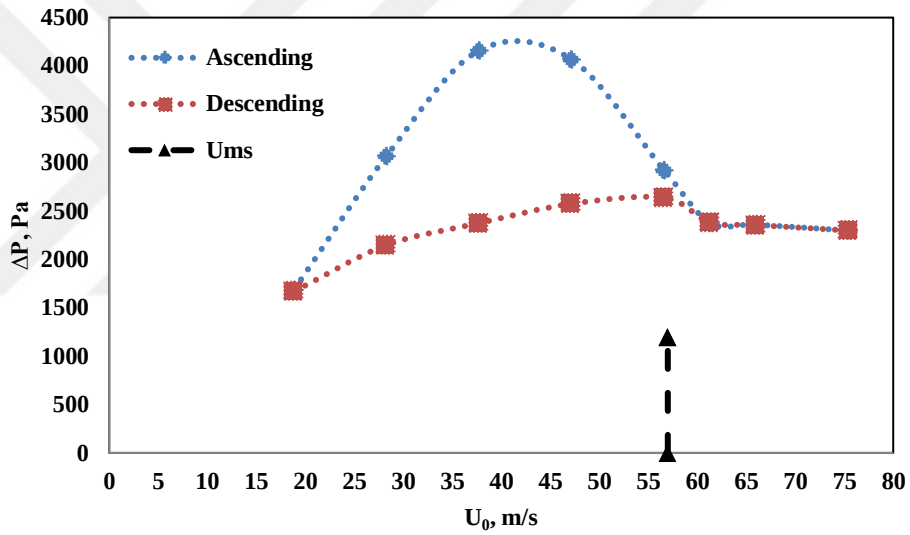

Figure 4.1 Bed pressure drop for alumina particles (H_b = 235 mm, γ = 31°)

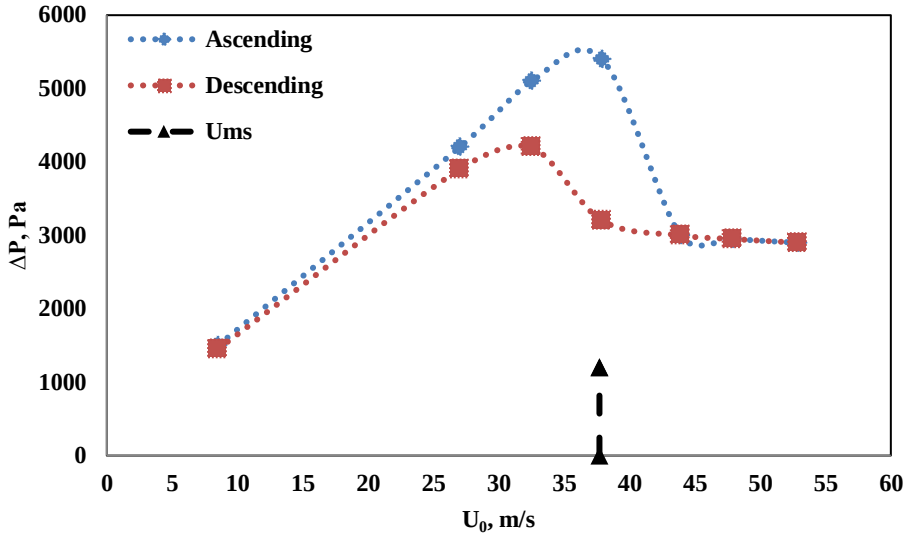

Figure 4.2 Bed pressure drop for glass beads (H_b = 144 mm, γ = 66º)

Table 4.1 Observed and recorded minimum spouting velocities (U_{ms}) in conical spouted beds

Particle	ρ_p (kg/m^3)	γ (º)	D_i (mm)	H_b (mm)	U_{ms} (m/s)	U_0/U_{ms}
Alumina	3700	45	12	140	56.40	1.25
Alumina	3700	45	15	140	36.80	1.25
Zirconia	6050	45	12	140	68.15	1.25
Zirconia	6050	45	15	140	45.31	1.25
Alumina	3700	60	12	100	44.64	1.25
Alumina	3700	60	15	100	30.20	1.25
Zirconia	6050	60	12	100	53.57	1.25
Zirconia	6050	60	15	100	38.07	1.25
Glass	2460	31	15	235	43.4	1.1
Alumina	3700	31	15	235	56.6	1.1
Zirconia	6050	31	15	235	64.6	1.1
Glass	2460	66	15	144	37.7	1.05
Alumina	3700	66	15	144	50.4	1.05
Zirconia	6050	66	15	144	57.5	1.05

4.2 Local flow structure measurements

In this thesis study, particle velocity and solids hold-up were measured in small and large-scale conical spouted beds with different cone angles operating with three different particles with varying densities (2460 kg/m^3 ≤ ρ_p ≤ 6050 kg/m^3) utilizing an optical fiber probe. The optical probe used in this study, allows the simultaneous measurement of local particle velocity and solids hold-up and thus local particle fluxes can be calculated. Particle flux is designated as the mass of particles passing per unit time and per unit area normal to the flow. It provides noteworthy information on particle flow dynamics (Kulah et. al. 2016). The following equation can be used for particle flux calculation:

$$G_s = U_p \varepsilon_s \rho_p \tag{4.1}$$

In order to ensure that experiments were performed in stable spouting operation, the spouting gas velocity was set to superficial gas velocity (U_0) which is higher than minimum spouting velocity (U_{ms}). The ratio of spouting gas velocity over minimum spouting velocity was set to 1.25 for small scale beds (45º and 60º) while for large scale beds (31º and 66º), it was 1.1 and 1.05, respectively, to ensure that the jet regime was not observed in the large scale spouted bed.

The experiments were carried out three times to conduct a reproducibility analysis, and the final data was obtained by taking average. The reproducibility analysis is discussed in detail in **Appendix**. For all measurements, the optical probe is inserted horizontally parallel to the conical base and radially moved along the particular port. In virtue of such settlement of optical probe, the measured particle velocity and flux can be termed as axial particle velocity and axial particle flux. In various operating conditions and using different bed materials, the particle velocity, solids hold-up and particle flux were measured by means of fiber optical probe.

4.2.1 Effect of Axial Position

In all the experiments, when the spouting gas was supplied to the system, it vertically accelerated the particles from the bed bottom. Accelerated particles gained their maximum velocity at the spout axis. As they rose up towards the bed surface, their velocity gradually decreased. From the spout center to the spout-annulus interface, particle velocity gradually decreased down to zero. Solids hold-up, on the other hand, gradually increased from spout center to the interface. At the interface, it sharply increased as the particles were suspended between the surrounding particles which were moving oppositely. In annulus region, a relatively more passive behaviour was observed. Particles moved downwards with a slow velocity generally between -0.01 m/s and -0.001 m/s. Solids hold-up fluctuated around loosely-packed solids hold-up value. **Figure 4.3** illustrates the significant change of the local flow structure in spout and annulus region. In the figure, there are two different y-axes indicating the parameter for spout and annulus regions individually. The arrows in each graph point the axes for corresponding regions. The error bars given on **Figure 4.3** indicate the variation in three experiments and show that the measurements were reproducible. As illustrated in the figure, the magnitude of the fluctuation in annulus measurements was higher compared to spout measurements.

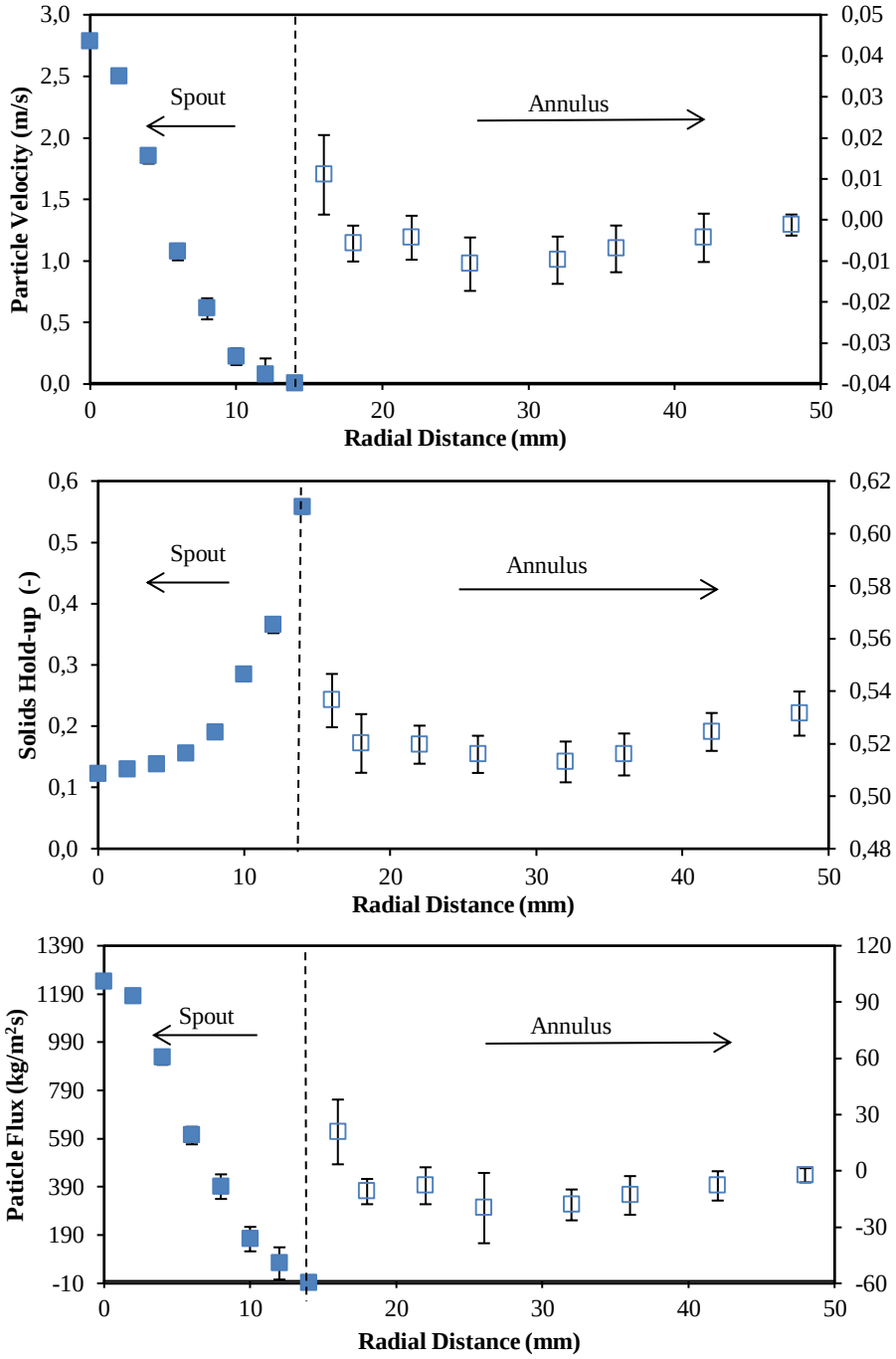

Figure 4.3 Radial profiles of local particle velocity, solids hold-up, and particle flux for alumina ($\gamma = 31°$, $z_2 = 128$ mm, $H_b = 168$ mm, $U_o = 1.1\ U_{ms}$)

The effect of axial position on local flow structure is illustrated in **Figures 4.4 and 4.5**. In the figures, it is clearly seen that in the spout region, the particle velocity decreased, solids hold-up and particle flux increased for both zirconia and glass particles from bed bottom to bed surface. This trend is in accordance with the profiles observed in previous studies (San Jose et al., 1998; Wang et al., 2009; Kulah et al., 2016). The solids hold-up and particle flux increases along the bed height due to entering of particles from the annulus to the spout. It can also be seen in **Figure 4.5** that the maximum particle velocity and flux were not measured exactly at the spout center for zirconia. This displacement of maximum particle velocity and flux position can be attributed to the radial movement of particles and their inter-collisions with each other in the spout (Krzywanski, 1992) This type of behaviour was also observed by He et al. (1994). The effect of axial position on local flow structure in the annulus was found to be insignificant. The increase in particle flux with axial height indicates an increase in lateral solids flow from the annulus to the spout.

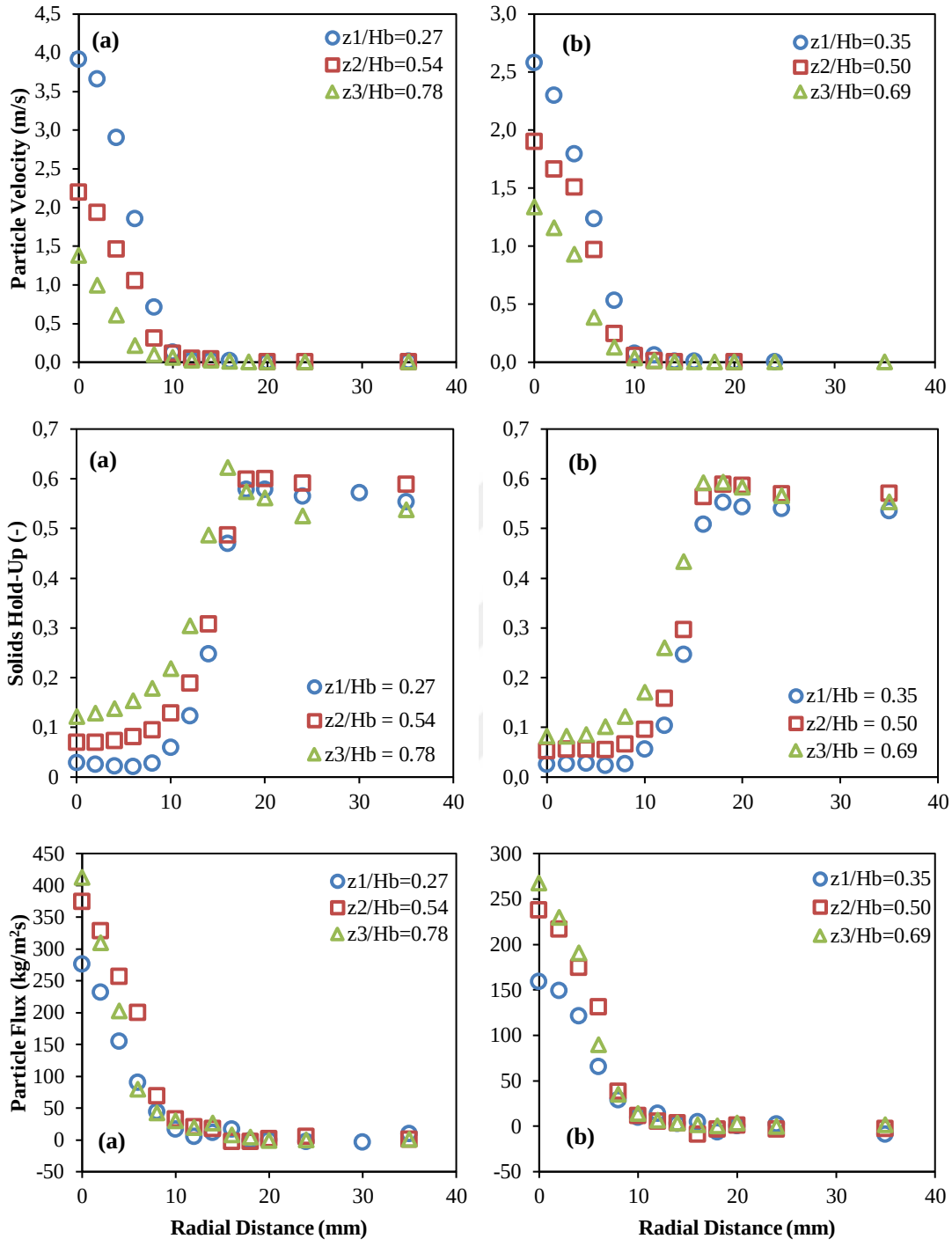

Figure 4.4 Effect of axial positions on local particle velocity, solids hold-up, and particle flux for glass (a) γ =31°, H_b =235 mm, U_o =1.1 U_{ms}, (b) γ =66°, H_b =144 mm, U_o =1.05 U_{ms}

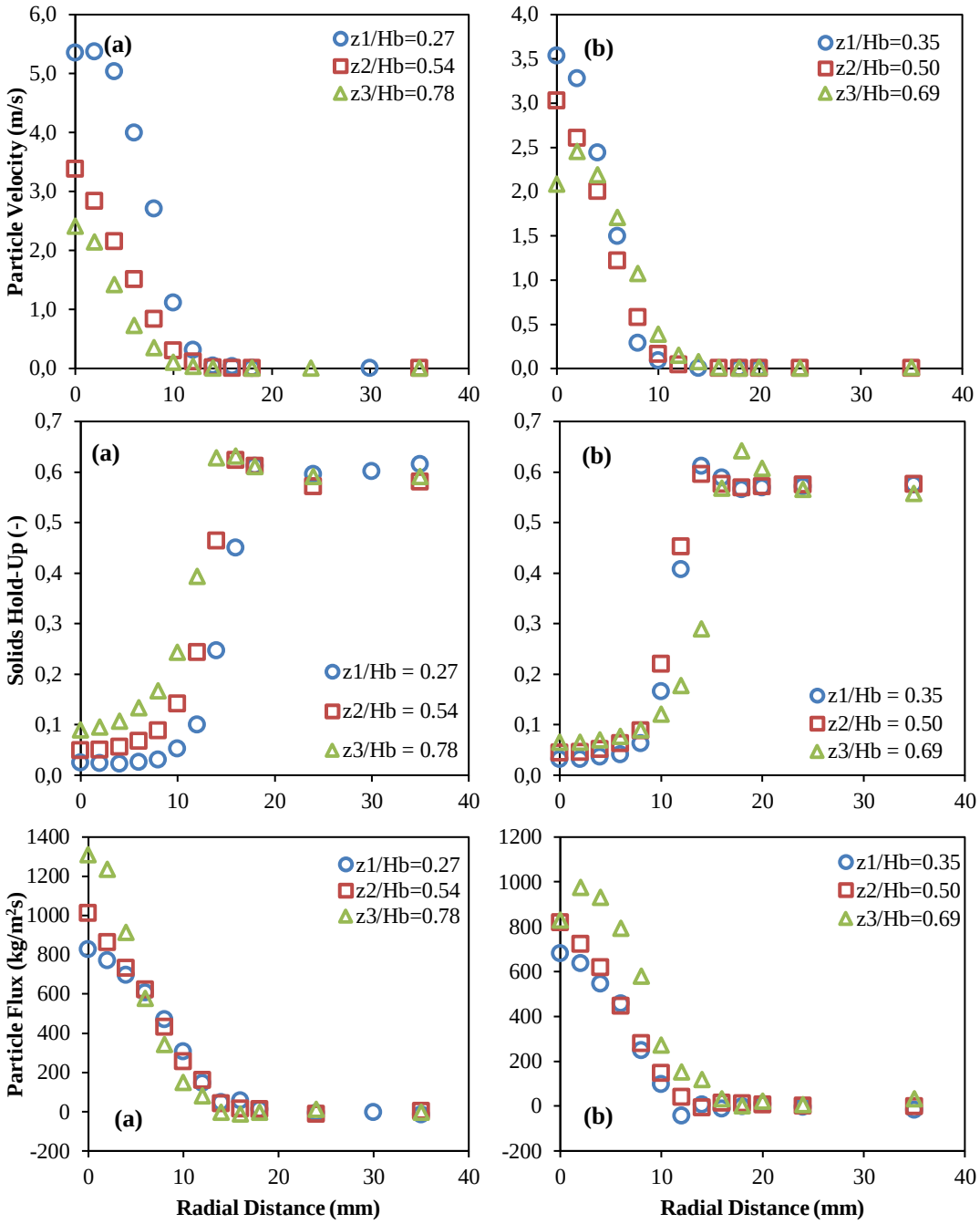

Figure 4.5 Effect of axial positions on local particle velocity, solids hold-up, and particle flux for zirconia (a) γ =31°, H_b =235 mm, U_o =1.1 U_{ms}, (b) γ =66°, H_b =144 mm, U_o =1.05 U_{ms}

4.2.2 Effect of Inlet Diameter

The effect of inlet diameter on particle normalized velocity, solids hold-up and particle flux is illustrated in **Figure 4.6**. Two different inlet diameters, 12 mm and 15 mm, were used in this study. Absolute particle velocities are higher for smaller inlet diameter because of that the U_{ms} values are higher for 12 mm inlet diameter (53.57 m/s and 44.64 m/s) than 15 mm inlet diameter (38.07 m/s and 30.20 m/s) for zirconia and alumina respectively. The reason why the U_{ms} is higher for smaller inlet diameters at the same gas flow rate can be addressed to that the jet formed in the spout is smaller and narrower but stronger, pushing the particles in upward direction with higher velocity. From the figure, it can be observed that the normalized velocity was higher for larger inlet diameters at this axial position for both zirconia and alumina particles. As for annulus, the changes were very minimal in terms of magnitude, similar to the finding of Olazar et al. (1998). Solids hold-up was not significantly influenced by the inlet diameter in spout and annulus regions despite small differences. Particle flux at the spout center was observed to be higher for smaller gas inlet nozzle mainly due to higher absolute particle velocity. As Spreutels et al. (2016) also recorded, particle circulation rate dropped with increasing gas-inlet diameter in parallel with the particle flux profile in the spout region demonstrated here. Through the spout-annulus interface and beyond of it, there was no substantial change in particle flux.

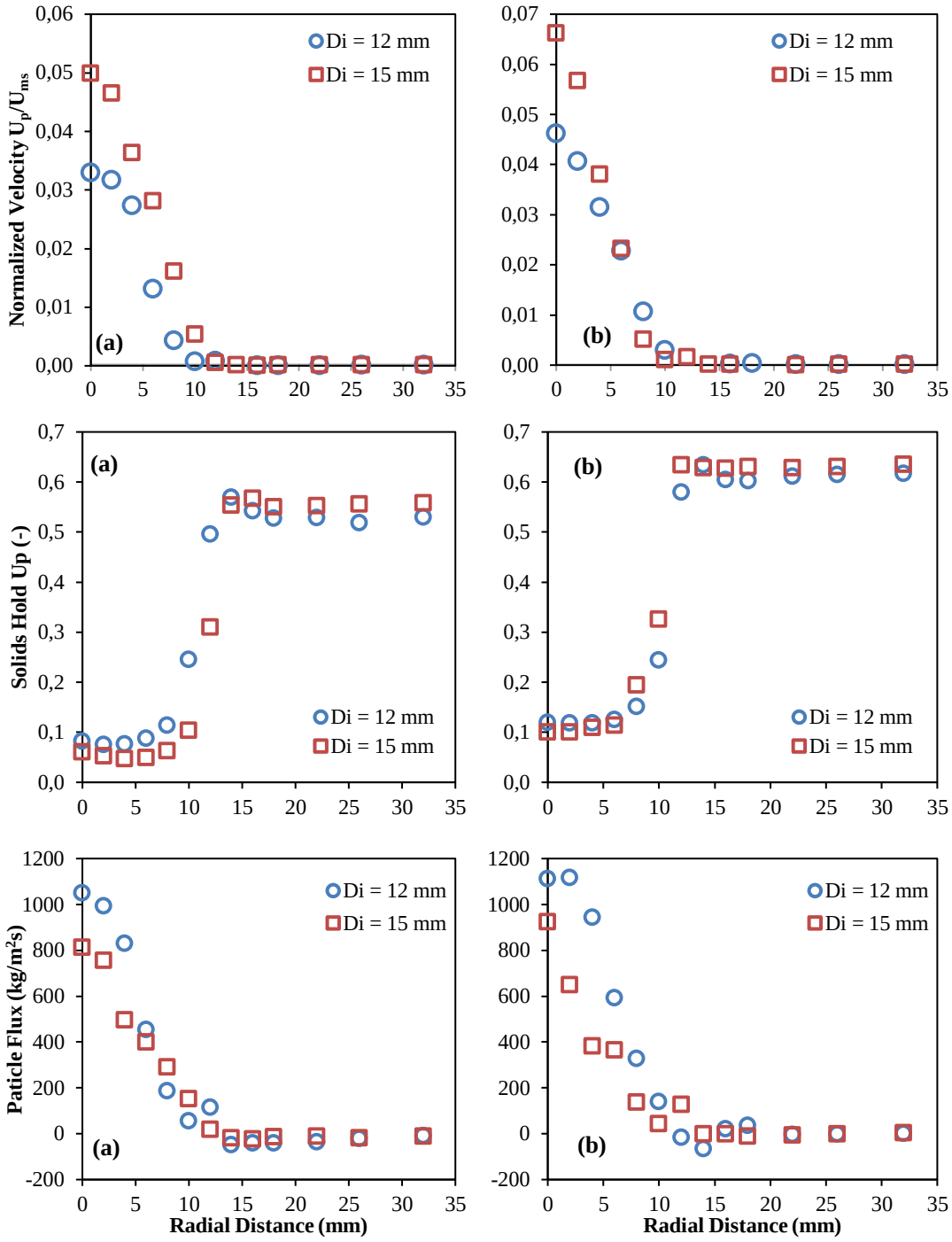

Figure 4.6 Effect of gas-inlet diameter on particle velocity, solids hold-up, and particle flux (γ =60°, z/H_b =0.5, U_o =1.25 U_{ms}, (a) Zirconia, (b) Alumina)

4.2.3 Effect of Cone Angle

Effect of conical angle on local time-mean particle velocity, solids hold-up and flux is illustrated in **Figures 4.7 and 4.8**. Owing to the design of two different spouted beds with different cone angles, the probe measurement heights are not equal to each other. In order to be able to make a comparison, the ratio of the measurement height to the static bed height (z/H_b) was set close to each other. Furthermore, since the U_{ms} values change with conical angle, the particle velocity was normalized by U_{ms}.

As can be seen in **Figure 4.7**, normalized velocities in spout region were higher for 31° bed for both glass and zirconia particles at the bottom section of the beds ($z/H_b \cong 0.3$). Annular region, on the other hand, was unaffected by the change of cone angle, as expected. No significant effect of cone angle on solids hold-up was observed in both spout and annulus regions. On the other hand, the particle flux increased with decreasing conical angle, due to higher local particle velocities measured at low conical angles. This effect was more pronounced for lighter particles compared to heavier particles. As illustrated in **Figure 4.8,** at upper axial positions of the bed ($z/H_b \cong 0.5$), no significant effect of cone angle on normalized particle velocities and solids hold-up was observed for both glass and zirconia particles. On the other hand, the particle flux increased with decreasing conical angle, due to higher local particle velocities measured at low conical angles. This effect is more pronounced for lighter particles compared to heavier particles.

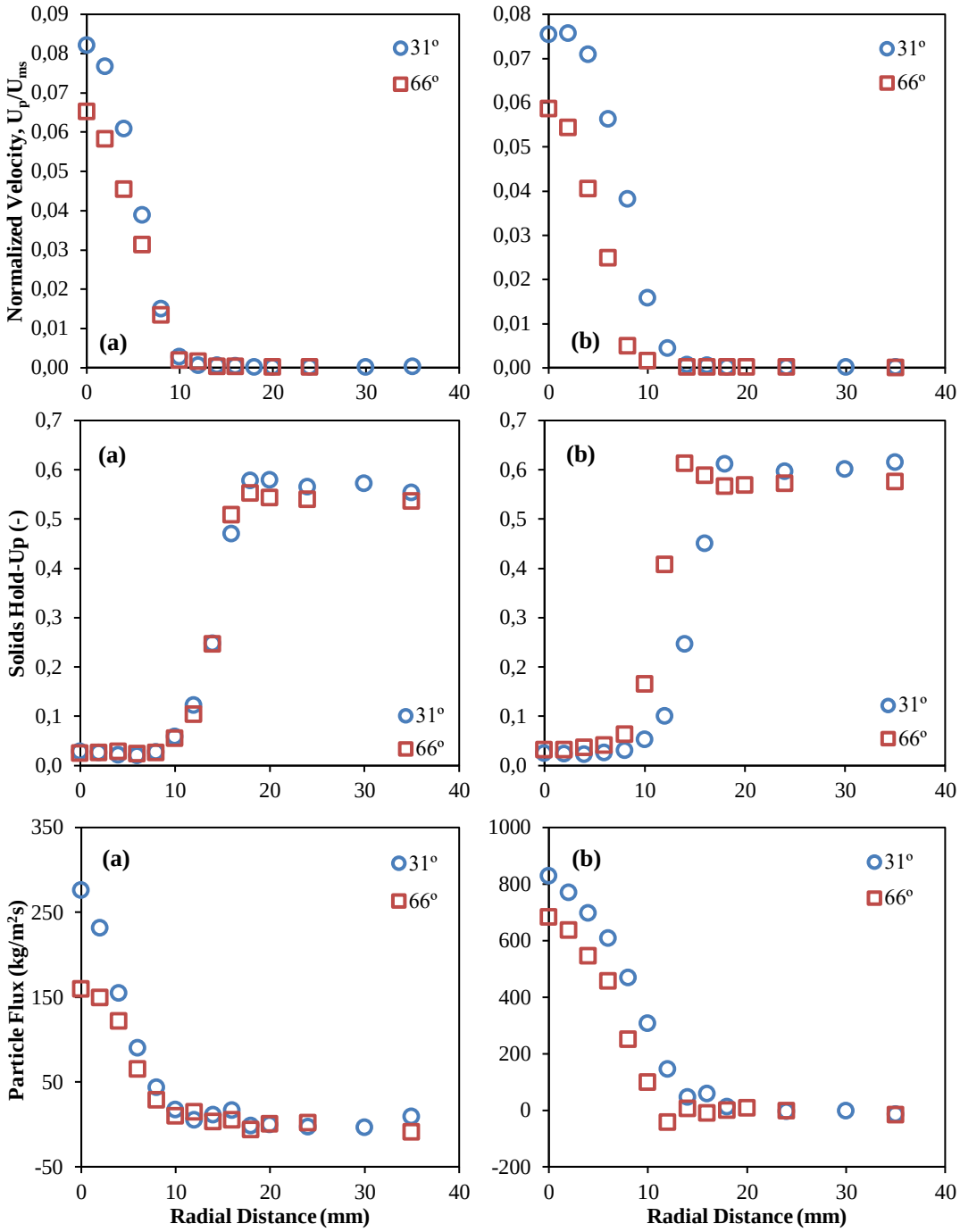

Figure 4.7 Effect of conical angle on radial profiles of local particle velocity, solids hold-up, and flux ($z_1/H_b = 0.27$ for $\gamma = 31°$, $z_1/H_b = 0.35$ for $\gamma = 66°$, (a) Glass (b) Zirconia)

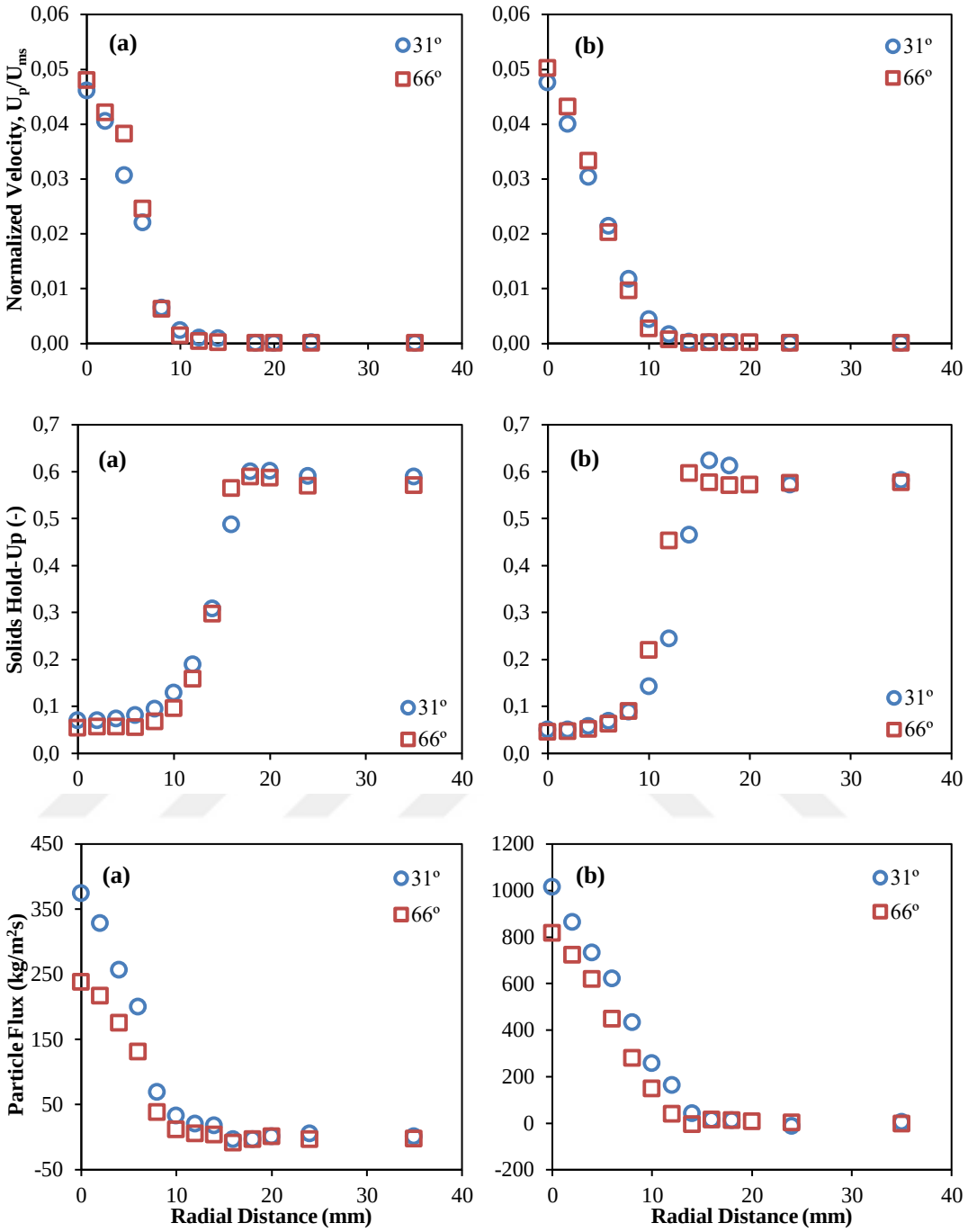

Figure 4.8 Effect of conical angle on radial profiles of local particle velocity, solids hold-up, and flux (z_2/H_b = 0.54 for γ = 31°, z_2/H_b = 0.50 for γ = 66°, (a) Glass (b) Zirconia)

4.2.4 Effect of Particle Density

Particle density is a prominent parameter having salient influence on bed hydrodynamics. As the U_{ms} values which are tabulated in **Table 4.1** are different for particles with varying density, to be able to make a comparison in common basis, normalized velocity term is plotted. In addition, the same measurement locations in 31° and 66° beds are chosen to eliminate the axial position effect. In **Figures 4.9 and 4.10**, the effect of particle density on the normalized particle velocity, solids hold-up and particle flux radial profiles are displayed.

Although the absolute particle velocities were higher for high-density particles, because of higher U_{ms} values, their normalized velocities were close to ones with low-density particles at the spout center. As for annulus, particles were in very slow downward motion, which is expected because of the nature of the flow in this region, therefore a tangible comparison was not possible. Solids hold-up profiles were found to be very similar in the spout for both light and heavy particles. Although the absolute particle velocities are different for different type of particles, due to different minimum spouting velocities, the internal jet is strong enough to prevent a significant lateral solid motion from annulus to the spout, which leads to very similar solids hold-up values for all particles at the spout center. Beyond the spout-annulus interface, solids hold-up values fluctuated around their loosely-packed solids hold-up values which are 0.63, 0.60 and 0.61 for glass, alumina and zirconia, respectively.

Particle flux is the most noticeably changed property by the particle density in the spout. The figure demonstrates that particle flux greatly increased as particle density increased in both 31° and 66° beds. This is caused by increase in U_{ms} as particle density increases. The results of this study are inconsistent with the literature study that was carried out with light particles ($65\ kg/m^3 \leq \rho_p \leq 2500\ kg/m^3$) where no trend in the change of solids circulation with particle density was observed evaluating the solid circulation (San Jose et al. 2006).

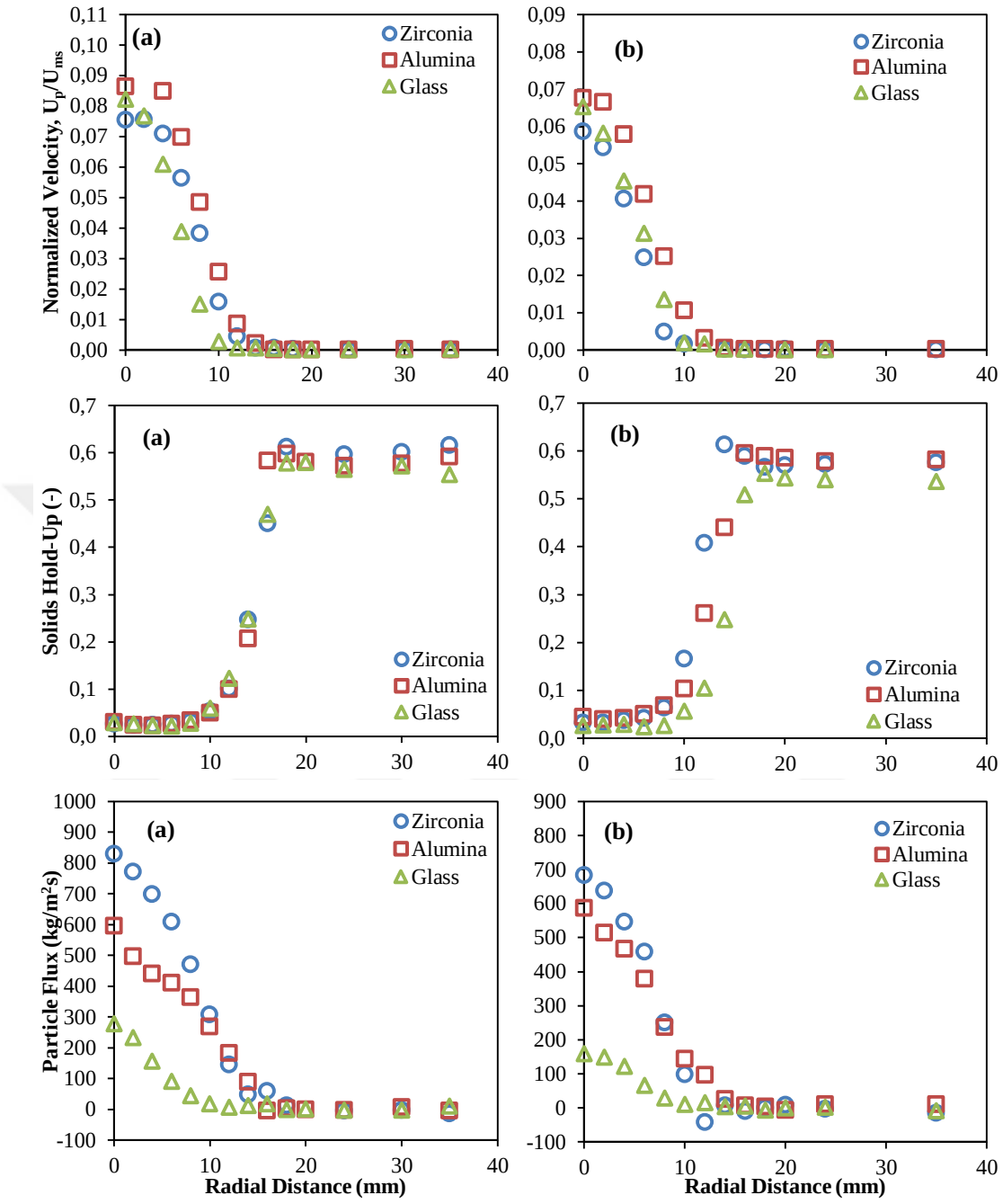

Figure 4.9 Effect of particle density on radial profiles of local particle velocity, solids hold-up, and flux ((a) $\gamma = 31°$, $z_1/H_b = 0.27$, $U_0/U_{ms} = 1.1$, (b) $\gamma = 66°$, $z_1/H_b = 0.35$, $U_0/U_{ms} = 1.05$)

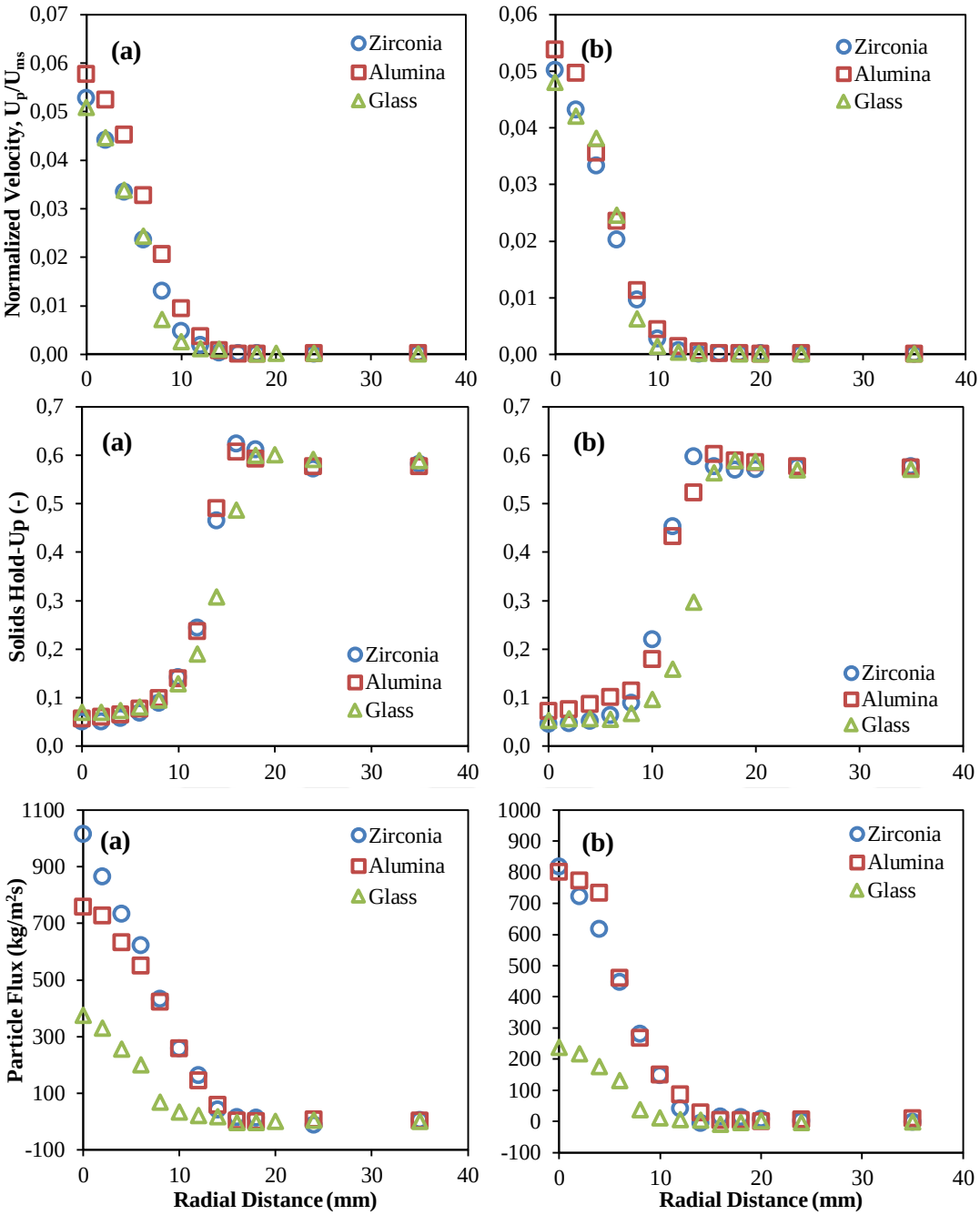

Figure 4.10 Effect of particle density on radial profiles of local particle velocity, solids hold-up, and flux ((a) $\gamma = 31°$, $z_2/H_b = 0.54$, $U_0/U_{ms} = 1.1$, (b) $\gamma = 66°$, $z_2/H_b = 0.50$, $U_0/U_{ms} = 1.05$)

4.3 Empirical Correlation

As discussed in previous sections, there are two clear regions in a spouted bed: Annulus and spout. The particles in the annulus region are in nearly loosely-packed state, and do not get affected significantly by the operating conditions and axial position. However, solids hold-up in the spout region is responsive to the changes in operating conditions. Therefore, the prediction of the change of solids hold-up in the spout region for various operating and design conditions is crucial. The only empirical equation for voidage profile prediction was proposed by San Jose et al. (2005). In this study, voidage correlations individually for spout center, bed wall and overall radial distribution (**Eq. 4.2, 4.6 and 4.7**, respectively) were developed.

$$\varepsilon(0) = \varepsilon(0)_{z=0.02} - E\left(\frac{z}{H_b}\right)^2 \tag{4.2}$$

$$\varepsilon(0)_{z=0.02} = 1 \qquad \text{for } \rho_p \geq \rho_g \tag{4.3}$$

$$\varepsilon(0)_{z=0.02} = \left(\frac{\rho_p}{\rho_g}\right)^{0.2} \qquad \text{for } \rho_p < \rho_g \tag{4.4}$$

$$E = 1.20\left(\frac{D_b}{D_i}\right)^{-0.12}\left(\frac{H_b}{D_o}\right)^{-0.97}\left(\frac{U_0}{U_{ms}}\right)^{-0.71}\gamma^{-0.19} \tag{4.5}$$

Here ε(0) indicates the voidage at the spout center (r = 0). According to their experimental observation, at z = 0.02 m, a height very close to the bed inlet, the bed voidage is unity. This is caused by solid cross-flow from annulus to spout and valid only for particles whose density is equal to or higher than glass beads, ρ_g, such as zirconia (6050 kg/m^3) or steel (7400 kg/m^3). It is, however, not unity for the particles lighter than glass beads because of solid cross-flow occurrence below z = 0.02 m (San Jose et al., 2005). The parameter *E* in **Eq. 4.5** was defined as a functional parameter that represents hydrodynamically important parameters such as bed diameter, bed bottom and bed inlet diameters, static bed height, ratio of superficial gas velocity-to-minimum spouting velocity and cone angle (San Jose et al. 1998). **Eq.**

4.6 and 4.7 are the correlations to predict the voidage at bed wall and at any radial distance, respectively.

$$\varepsilon(w) = \varepsilon_0 \left(1 + \frac{H_b - z}{H_b}\right)^{0.5} \tag{4.6}$$

$$\varepsilon = \frac{\varepsilon(0) - \varepsilon(w)}{1 + \exp((r - r_s)/27.81 r_s^{2.41})} + \varepsilon(w) \tag{4.7}$$

It must be noted that San Jose et al. (2005) developed these correlations by using only light particles with varying densities (65 kg/m^3 ≤ ρ_p ≤ 2420 kg/m^3). Therefore, in this study, a new correlation is developed to predict solids hold-up at the spout center for both light and heavy particles. The data set used and the procedure is explained below.

4.3.1 Correlation Development

This proposed correlation was developed by utilizing all the experimental data obtained in this study and the ones reported in the literature. Experimental conditions of literature data that were used in this correlation are given in **Table 4.2**. Only the solids hold-up values at the spout center were used. From this data set, 51 data out of 60 were arbitrarily chosen to develop the correlation. Remaining 9 data (15%) was saved for usage in the validation of the correlation.

Table 4.2 Literature studies and corresponding conditions for correlation development

Study	Particle Type	Bed geometry	z/H_b
Olazar et al. (1995)	Glass (d_p = 4 mm, ρ_p = 2420 kg/m^3)	γ = 33°; D_c = 0.36 m	0.11, 0.28, 0,45, 0.67
San Jose et al.(1998)	Glass (d_p = 3, 4, 5 mm, ρ_p = 2420 kg/m^3)	γ = 33, 36, 45°; D_c = 0.36 m	0.11, 0.28, 0,45, 0.67
San Jose et al. (2005)	Glass (d_p = 3.5 mm, ρ_p = 2420 kg/m^3)	γ = 33°; D_c = 0.36 m	0.11, 0.28, 0,45, 0.67
Aradhya et al. (2017)	Glass, Steel (d_p = 1.09 mm, ρ_p = 2500 kg/m^3, 7400 kg/m^3)	γ = 60°; D_c = 0.076, 0.152 m	0.37

The term $\varepsilon(0)_{z=0.02}$ is set to unity in this study because the densities of all particles are equal to or higher than the density of glass beads (2420 kg/m^3). Considering the conversion from voidage to solids hold-up, the solids hold-up will be exactly equal to the absolute value of the second term in **Eq 4.2**. For simplification, the term *E* in **Eq. 4.5** was substituted in **Eq. 4.2** and the entire correlation system was reduced to a one single expression as follows.

$$\varepsilon_s(0) = 0.043\,(\frac{D_b}{D_i})^{0.169}(\frac{H_b}{D_o})^{0.435}(\frac{U_0}{U_{ms}})^{0.890}(\frac{z}{H_b})^{0.816}\gamma^{-0.646} \qquad (4.8)$$

Similar to the study done by San Jose and co-workers (2005), non-linear regression method was used to develop the correlation. **Figure 4.11** shows the comparison of the predicted and experimentally measured solids hold-up values for both the original correlation of San Jose et al. (2005) and correlation developed in this study. It should be noted that for comparison in the figure 9 data points, which were not included in the correlation development, were used. The experimental conditions of these data points are given in **Table 4.3**.

As far as new correlation is concerned, calculated values of solids hold-up display an acceptable level of prediction with an average deviation of 40%. The correlation brings more accurate center solids hold-up predictions compared the original correlation.

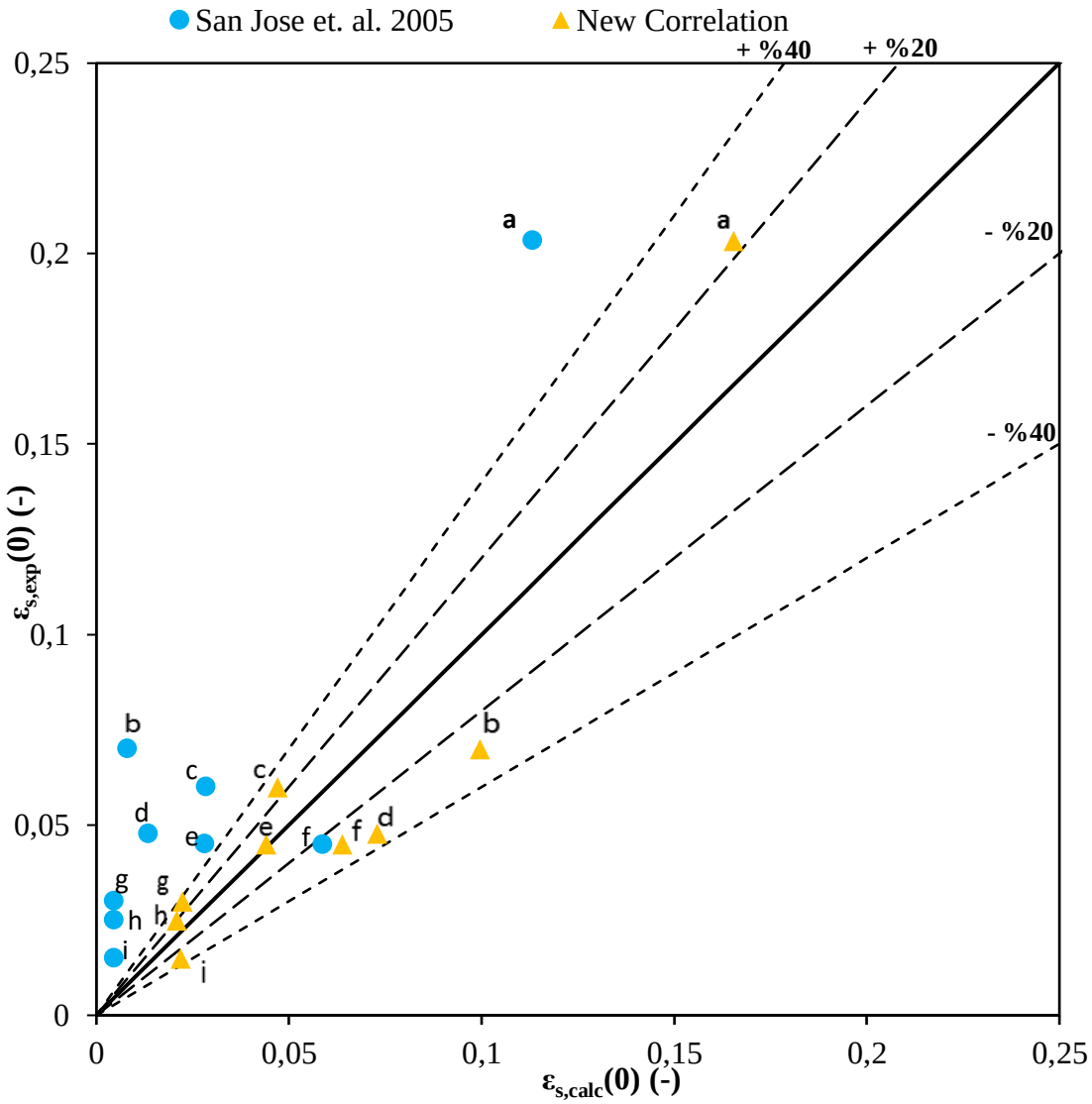

Figure 4.11 Comparison of experimental and calculated values of solids hold-up at the spout center

Table 4.3 Experimental conditions of validation data

	Reference	Particle	γ(°)	D_i (mm)	z/H_b
a	This study	Zr	45	15	0.85
b	Aradhya et al. 2017	Glass	60	19	0.37
c	Olazar et al. 1995	Glass	33	30	0.28
d	This study	Zr	45	12	0.3
e	San Jose et al. 1998	Glass	36	30	0.28
f	This study	Zr	66	15	0.5
g	San Jose et al. 2005	Glass	33	30	0.11
h	San Jose et al. 1998	Glass	36	30	0.11
i	San Jose et al. 1998	Glass	33	30	0.11

Figure 4.12 shows the comparison of the calculated and measured radial solids-hold up distribution in a conical spouted bed. The experimental data was retrieved from the study of Wang et al. (2009). For *New Correlation* curve, to predict the solids hold-up for intermediate radial points and at bed wall, the **Eq. 4.6 and 4.7** were used, as proposed by San Jose et al. (2005). The figure shows that new correlation gives more accurate prediction than the one developed by light particles only.

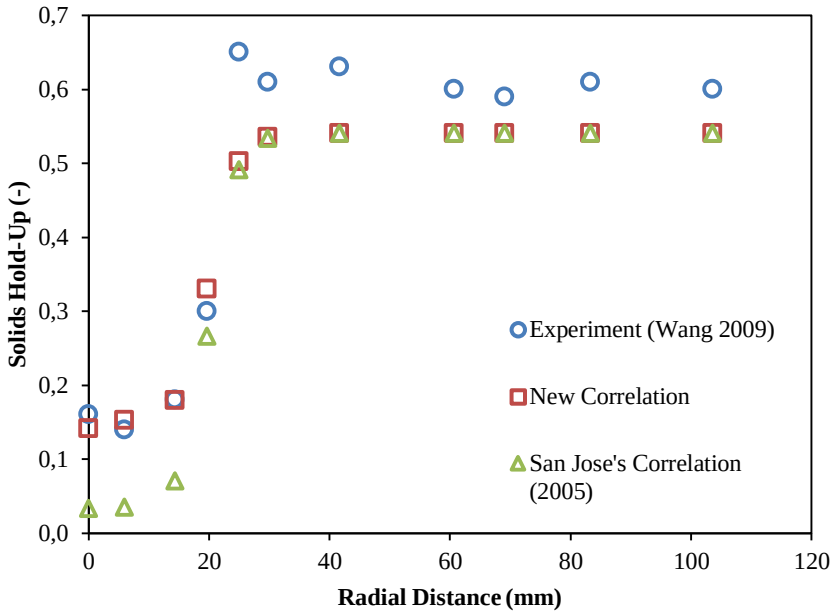

Figure 4.12 Comparison of experimental and correlated local solids hold-up values ($\gamma = 45°$, $d_p = 1.16$ mm glass beads, $z/H_b = 0.61$)

4.4 Effect of Fluidizing Gas – Spout-Fluid Operation

In conical spouted beds, the effect of fluidizing gas (Q_f) is a parameter not investigated before for local particle properties. The introduction of the fluidizing gas through the conical walls changes the system from conical spouted bed to conical spout-fluid bed. Thus, dead zones and agglomeration problems in reactor applications can be minimized, and better gas-solid contact can be potentially provided (Epstein and Grace, 2011). In this regard, the effect of fluidizing gas was investigated by choosing two different flow rates through the conical walls. These flow rates were identified as “minimum” and “maximum”. In the spout-fluid bed operation, it is known that the introduction of the fluidizing gas decreases the minimum spouting velocities (Yaman, 2017). The reduction in U_{ms} is because of easier aeration of loosely-packed particles by fluidizing gas. So, the term “minimum” corresponds to the first point at which U_{ms} is lowered distinctly as the fluidizing gas velocity is gradually increased. On the other side, the maximum fluidizing gas flow

rate was chosen according to the criteria, for which spouting stability should not be affected and bubble formation in the annulus should not be observed.

The experiments were carried out based on increase of total gas flow rate (Q_t). During the experiments, the spouting gas flow rate (Q_0) remains constant, while the fluidizing gas flow rate increases. The increase in fluidizing air is shown as Q_f/Q_t, the ratio of fluidizing air flow to total air flow. In **Table 4.4**, the experimental conditions and corresponding spouting gas together with fluidizing gas flow rates are given.

Table 4.4 Fluidizing gas flow rates used in spout-fluid bed experiments

γ (°)	Particle	Q_{ms} (m^3/min)	Q_0 (m^3/min)	Q_f (m^3/min)	Q_{total} (m^3/min)	Q_f/Q_t
31	Al	0.45	0.49	$Q_{f,min}$ = 0.16	0.65	0.25
		0.45	0.49	$Q_{f,max}$ = 0.38	0.87	0.44
66	Al	0.54	0.57	$Q_{f,min}$ = 0.17	0.74	0.23
		0.54	0.57	$Q_{f,max}$ = 0.35	0.92	0.38
66	Zr	0.61	0.64	$Q_{f,min}$ = 0.15	0.79	0.19
		0.61	0.64	$Q_{f,max}$ = 0.40	1.04	0.38

In **Figure 4.13**, particle velocity, solids hold-up and particle flux measurements in spout-fluid operation are illustrated for alumina and zirconia. During the zirconia experiments, it was observed that when the optical probe was approached near the spout center (r = 0 and 2 mm), the stable spouting regime was ceased by exhibiting a pulsative behaviour, which led optical probe unable to take measurements. The figure demonstrates that the particle velocities are not significantly affected by fluidizing gas flow in the spout region. The solids hold-up is observed to be slightly lower compared to spouted bed operation where there is no fluidizing gas (Q_f = 0). Since the fluidizing gas pushes the particles at the wall to the center, the annulus region is considered to be slightly more dynamic resulting in lower solids hold-up. However, solids hold-up does not further decrease as the fluidizing gas flow rate changes from $Q_{f,min}$ to $Q_{f,max}$. As for particle flux, it has a slight increase in spout region and the overall change is not remarkable.

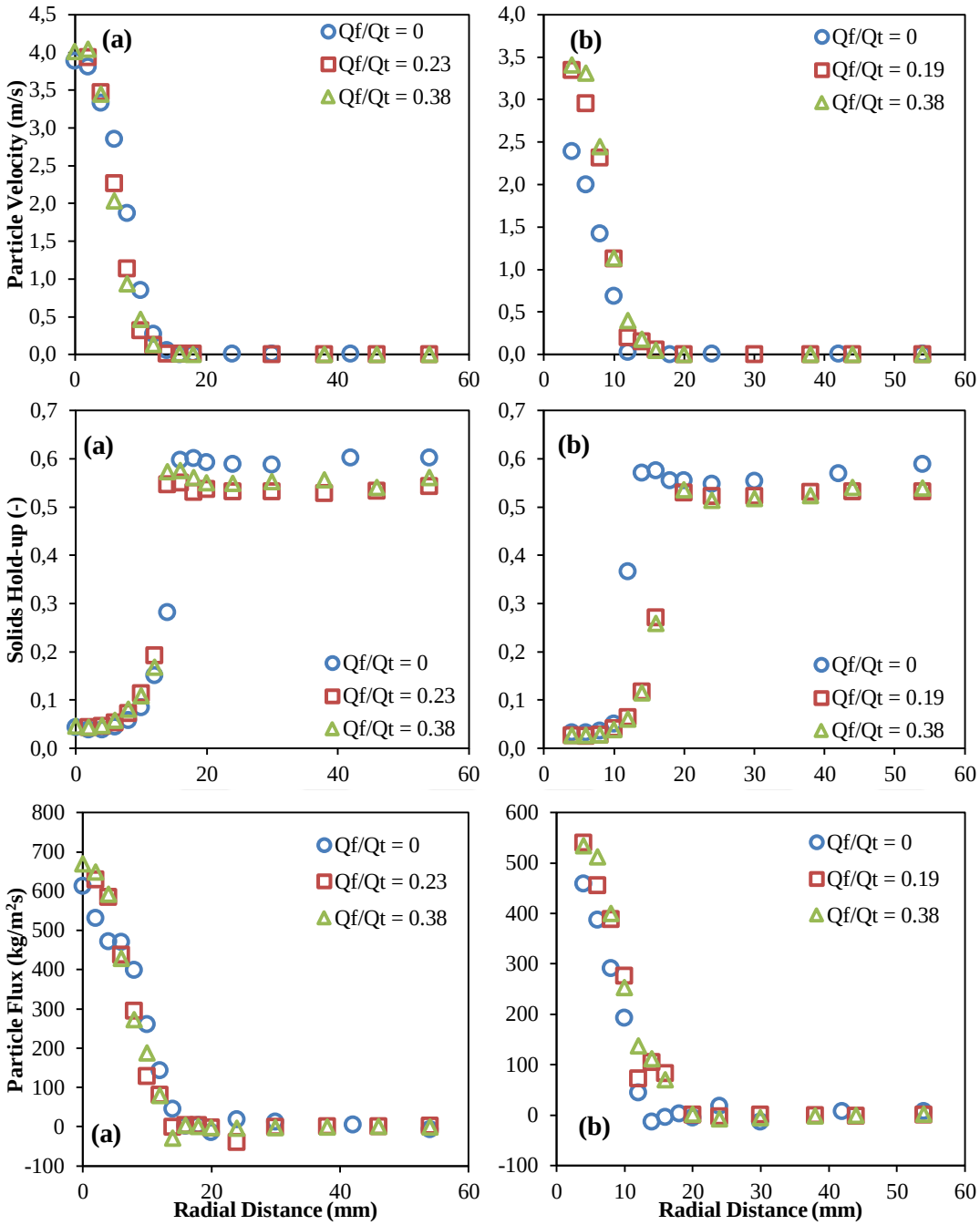

Figure 4.13 Effect of fluidizing gas on local particle velocity, solids hold-up and particle flux ($\gamma = 66°$, $z_1 = 50$ mm, $H_b = 144$ mm, $U_0/U_{ms} = 1.05$ ($Q_t = Q_0 + Q_f$), (a) Alumina (b) Zirconia

CHAPTER 5

CONCLUSIONS

This study was conducted as an investigation of local flow structure in conical spouted and spout-fluid beds operating with low- and high-density particles. The experiments were performed in small-scale (D_c = 150 mm) and large-scale (D_c = 250 mm) bed systems with various cone angles (31°, 45°, 60° and 66°). An optical probe was used to measure particle velocity, solids hold-up and particle flux as an indication of local flow structure. 1 mm sized low- and high-density particles (glass beads, alumina and zirconia) were used. The effects of bed design parameters (such as inlet diameter and conical angle) and operating conditions (such as particle density, axial height of measurement and fluidization gas flow rate) on the local particle flow characteristics were investigated in detail. An empirical correlation was proposed for solids hold-up prediction at the spout center based on the findings of experimental outcome of this work and literature studies. The following conclusions can be stated based on the experimental analysis carried out in this work:

- Spout and annulus regions show different flow behaviour in terms of particle velocity and solids hold-up under the effects of investigated parameters The flow in the annulus is characterized by loosely packed bed with slight particle down-flow whereas the spout region has an upward gas-solid flow with decreasing particle velocity and increasing solids hold-up along the axis. Particles acquire a maximum velocity at the spout axis with a

radially decreasing trend towards the spout-annulus interface, finally reaching zero and negative (downwards direction) values in the annulus.

- Particle velocity, solids hold-up and particle flux are significantly affected by the change in axial position for spout region only. In bottom spout area, higher particle velocities are measured with lower solids hold-up whereas top spout area has relatively slower particles in a denser solid medium. Regardless of bed material and bed cone angle, noticeably more solid circulation is observed in higher axial positions due to lateral motions of solids from the annulus to the spout.
- Cone angle does not significantly affect the solids hold-up. Particle flux on the other side, decreases with increasing cone angle and it is more influential for glass beads as the lightest particle used in this work.
- Particle density has no pronounced effect on solids hold-up in both spout and annulus regions. Normalized velocities are observed to be close to each other in 31° and 66° beds. As for particle flux, it is significantly increased with increasing particle density in the spout region.
- Introduction of fluidizing gas, an operating system in spout-fluid mode, does not change the local flow structure significantly. The increase in total gas flow in spout-fluid beds, i.e. further increase in fluidizing gas flow does not change the flow properties, regardless of particle density.

In the light of these findings, one can conclude that using low conical angles can be more feasible for an industrial scale spouted bed reactor design in order to achieve higher particle circulation and thus reaction efficiency. The gas-solid flow dynamics in spouted beds operated with high density particles is found to be similar to that operated with relatively light particles. With the spout-fluid bed operation, although the total gas flow rate through the bed increases substantially, no significant change is observed in the gas-solid flow behaviour.

5.1 Suggestions for Future Work

This study involves the local flow structure of high-density particles having 1 mm diameter. In this respect, the particle size can be a parameter to investigate. Considering Geldart's classification, the particle size and density can be investigated in a wider range, which is applicable in spouted bed systems.

REFERENCES

Ali, N., Al-Juwaya, T., Al-Dahhan, M. (2016). Demonstrating the non-similarity in local holdups of spouted beds obtained by CT with scale-up methodology based on dimensionless groups. *Chemical Engineering Research and Design, 114*, 129–141.

Aradhya, S., Taofeeq, H., Al-Dahhan, M. (2017). Evaluation of the dimensionless groups based scale-up of gas–solid spouted beds. *International Journal of Multiphase Flow, 94*, 209–218.

Berruti, F., Muir, J. R., Behie, L.A. (1988). Solids Circulation in a Spout Fluid Bed with Draft Tube. *Can. J. Chem. Eng., 66*, 919-923.

Chatterjee A. (1970). Spout-Fluid Bed Technique. *Ind. Eng. Chem. Process Des. Develop. 9, 2*, 340-341.

Chatterjee, A. R. R., Adusumilli, S., & Deshmukh, A.V. (1983). Wall-to-bed heat transfer characteristics of spouted-fluid beds. *Can. J. Chem. Eng., 61*, 390–397.

Choi, M., Meisen, A. (1992). Hydrodynamics of shallow, conical spouted beds. *Can. J.Chem. Eng., 70*, 916-24.

Duarte, C. R., Murata, V.V., Barrozo, M. A. S. (2008). Experimental and Numerical Study of Spouted Bed Fluid Dynamics. *Brazilian Journal of Chemical Engineering. 25, 01*, 95 – 107.

Elordi, G., Olazar M., Aguado R., Lopez, G., Arabiourrutia, M., Bilbao, J. (2007) Catalytic pyrolysis of high density polyethylene in a conical spouted bed reactor, *Journal of Analytical and Applied Pyrolysis, 79*, 450–455.

Epstein, N., & Grace, J.R. (2011). Spouted and spout-fluid beds: Fundamentals and applications. New York: Cambridge University Press.

Golshan, S., Yeniceri, A., Zarghami, R., Mostoufi, N., Koksal, M., Kulah, G. (2017). Effects of particle density and gas inlet diameter on particle velocity, solids hold-up and particle flux distributions in conical spouted beds with high density particles. 7th International Symposium on Spouted Beds (ISSB-7), Barcelona, Spain, October 1-5, 2017.

He, Y.L., Qin, S.Z., Lim, C.J., Grace, J.R. (1994). Particle velocity profiles and solid flow patterns in spouted beds. *Can. J. Chem. Eng., 72*, 561-568.

Kirbas, G. (2004). Solid motion and mixing in high-density circulating fluidized beds, Doctoral dissertation, Ph. D. Thesis, University of British Columbia, Vancouver, Canada.

Kmiec, A. (1980). Hydrodynamics of flows and heat transfer in spouted beds. *Chem. Eng. J., 19,* 189–200.

Krzywanski, R. S. (1992). Multi-Dimensional Modelling of a Spouted Bed, Doctoral dissertation, Ph. D. Thesis, University of British Columbia, Vancouver, Canada.

Kulah, G., Sarı, S., Koksal, M. (2016). Particle Velocity, Solids Hold-Up, and Solids Flux Distributions in Conical Spouted Beds Operating with Heavy Particles. *Industrial & Engineering Chemistry Research, 55*, (11): 3131-3138.

Kunii, D., & Levenspiel, O. (1991). Fluidization engineering, 2nd ed. New York: John Wiley and Sons.

Mathur K. B. and Gishler P. E. (1955). A technique for contacting gases with coarse particles. *AIChE Journal, 1*, 157–164.

Nagashima, H., Kawashiri, Y., Suzukawa, K., Ishikura, T. (2015). Effects of Operating Parameters on Hydrodynamic Behavior of Spout-Fluid Beds without and with a Draft Tube. *Procedia Engineering 102*, 952 – 958.

Olazar, M., San Jose, M. J., Llamosas, R., Bilbao, J. (1994). Hydrodynamics of sawdust and mixtures of wood residues in conical spouted beds. *Ind. Eng. Chem. Res., 33*, 993-1000.

Olazar, M., San Jose, M. J., Llamosas, R., Alvarez, S., Bilbao, J. (1995). Study of Local Propertiesin Conical Spouted Beds Using an Optical Fiber Probe. *Ind. Eng. Chem.Res. 34*, 4033-4039.

Olazar, M., San Jose, M. J., Llamosas, R., Alvarez, S., Bilbao, J. (1998). Measurement of Particle Velocities in Conical Spouted Beds Using an Optical Fiber Probe. *Ind. Eng. Chem. Res. 37*, 4520-4527.

Olazar, M., San Jose, M. J., Izquierdo, M.A., Salazar, A.O., Bilbao, J. (2001). Effect of operating conditions on solid velocity in the spout, annulus and fountain of spouted beds. *Chemical Engineering Science. 56*, (11): 3585-3594.

Pianarosa, D. L., Freitas, L., Lim, C.J., Grace, J. R., Dogan, O.M. (2000). Voidage and Particle Velocity Profiles in a Spout-Fluid Bed. *Can. J. Chem. Eng., 78,* 132-142.

Santos, D. A., Alves, G. C., Duarte, C. R.,, Barrozo, M. A. S. (2012) Disturbances in the Hydrodynamic Behavior of a Spouted Bed Caused by an Optical Fiber Probe: Experimental and CFD Study. *Ind. Eng. Chem. Res. 51*, 3801-3810.

San Jose, M.J., Olazar, M., Alvarez, S., Bilbao, J. (1998a). Local bed voidage in conical spouted beds. *Ind. Eng. Chem. Res.. 37,* (6): 2553-2558.

San Jose, M.J., Olazar, M., Alvarez, S., Izquierdo, M.A., Bilbao, J. (1998b). Solid cross- flow into the spout and particle trajectories in conical spouted beds, *Chem Eng Sci, 53*: 3561–3570.

San Jose, M.J., Olazar, M., Alvarez, S., Bilbao, J. (2005). Local porosity in conical spouted beds consisting of solids of varying density. *Chem Eng Sci, 60*, 2017–2025.

San Jose, M. J., Alvarez, S., Morales, A., Olazar, M., Bilbao, J. (2006). Solid Cross-flow into the spout and particle trajectories in conical spouted beds consisting of solids of different density and shape. *Chemical Engineering Research and Design, 84*, (A6): 487-494.

Sarı, S., Çangal, P., Külah, G., Köksal, M. (2011). Taşkın Yatak Nükleer Yakıt Kaplayıcılarının Hidrodinamik Özelliklerinin İncelenmesi, TÜBİTAK Proje No: 108M435.

Sarı, S., Kulah, G., Koksal, M. (2012). Characterization of gas-solid flow in conical spouted beds operating with heavy particles. *Exp. Therm. Fluid Sci., 40*, 132−139.

Spreutels, L., Haut, B., Legros, R., Bertrand, F., Chaouki, J. (2016). Experimental investigation of solid particles flow in a conical spouted bed using radioactive particle tracking. *AIChE, 62*, 26-37.

Stocker, R. K., Eng, J. H., Svrcek, W. Y., Behie, L. A (1989). Ultrapyrolysis of propane in a spouted-bed rector with a draft tube. *AIChE J., 35*, 1617–1624.

Sutanto, W., Epstein, N., Grace, J.R. (1985). Hydrodynamics of Spout-Fluid Beds. *Powder Technology, 44*, 205 – 212.

Van Velzen, D., Flamm, H.J., Langenkamp, H., Casile, A. (1974). Motion of solids in spouted beds. *Can. J. Chem. Eng., 52* (2): 156-161.

Wang, Z., Bi, H.T., Lim, C.J., Su, P. (2004). Determination of minimum spouting velocities in conical spouted beds, *Can. J. Chem. Eng., 82*, 11–19.

Wang, Z., (2006). Experimental Studies and CFD Simulations of Conical Spouted Bed Hydrodynamics, Doctoral dissertation, Ph. D. Thesis, University of British Columbia, Vancouver, Canada.

Wang, Z., Bi, H. T., Lim, C. J. (2009). Measurements of Local Flow Structures of Conical Spouted Beds by Optical Fibre Probes. *Can. J. Chem. Eng., 87*, 264-273.

Yaman, O. (2017). Bed-to-surface heat transfer in conical spouted and spout–fluid beds, Master of Science Thesis, Department of Chemical Engineering, Middle East Technical University, Ankara, Turkey.

APPENDIX

A.1 Reproducibility of Local Flow Structure Measurements

The experiments were performed three times and the measurement results were plotted as radial profiles of particle velocity, solids hold-up and particle flux in **Figures A.1 and A.2**.

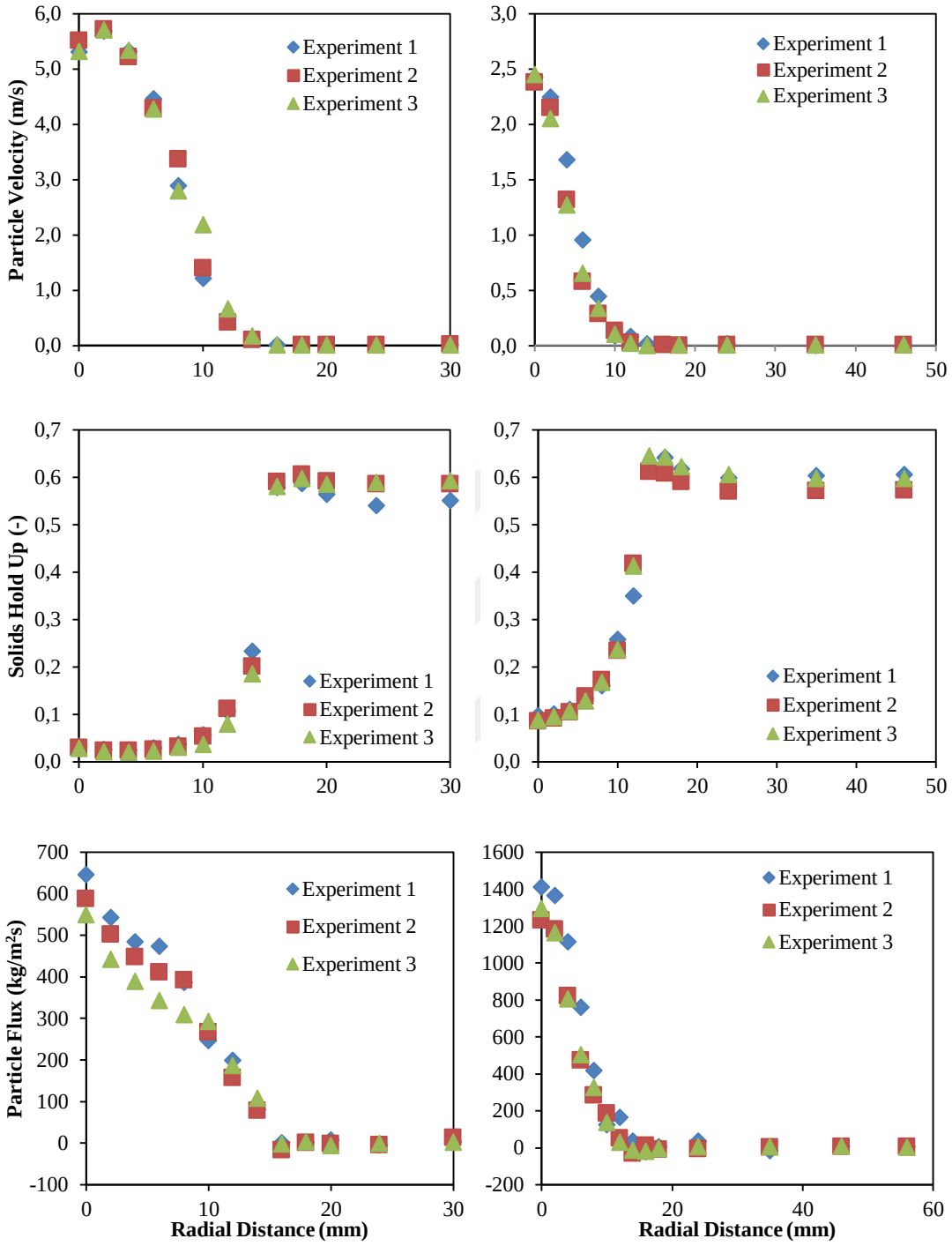

Figure A.1 Particle velocity, solids hold-up and particle flux distributions (a) Alumina, 31°, $z_1/H_b = 0.27$, (b) Zirconia, 31°, $z_2/H_b = 0.78$)

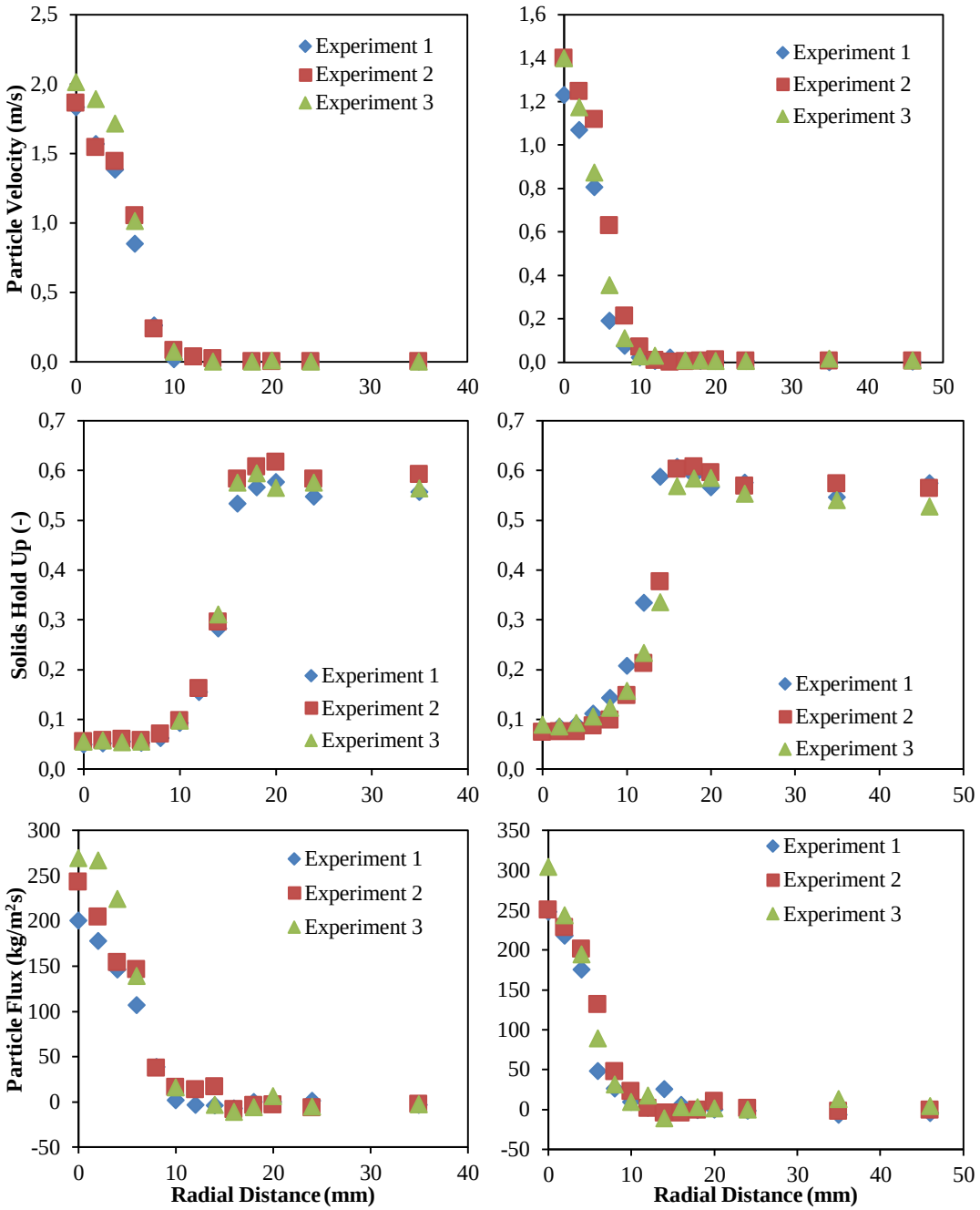

Figure A.2 Particle velocity, solids hold-up and particle flux distributions (a) Glass, 66°, $z_2/H_b = 0.50$, (b) Glass, 66°, $z_3/H_b = 0.70$)